

Mathematical Modelling of Differential Equations and its Applications in Biomedical Industry

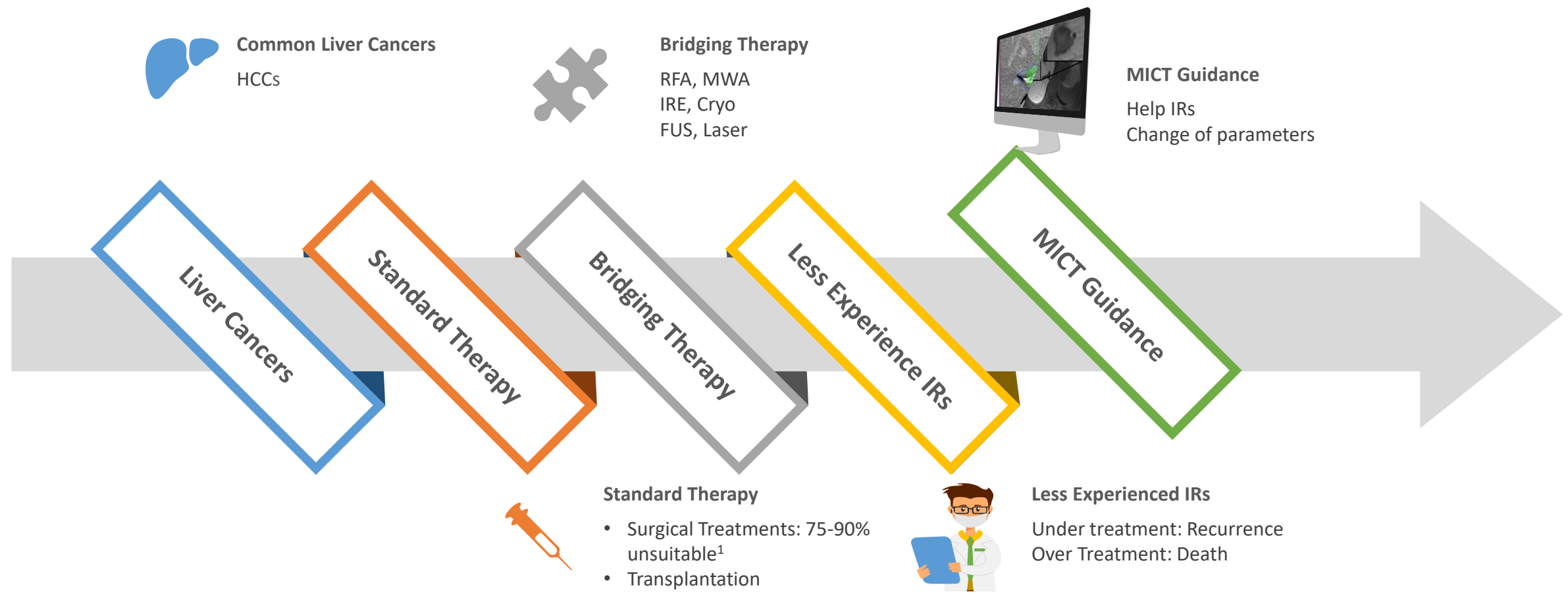
Panchatcharam Mariappan

Associate Professor

**Department of Mathematics and Statistics,
IIT Tirupati**

Recap

Cancer Treatments



1. Bruix J, Sherman M (2011) Management of hepatocellular carcinoma: an update. Hepatology 53(3):1020–1022

Image Sources: <https://angiodynamics.com>
<https://http://www.mermaidmedical.dk/>

Patient-, Device-Specific Parameters

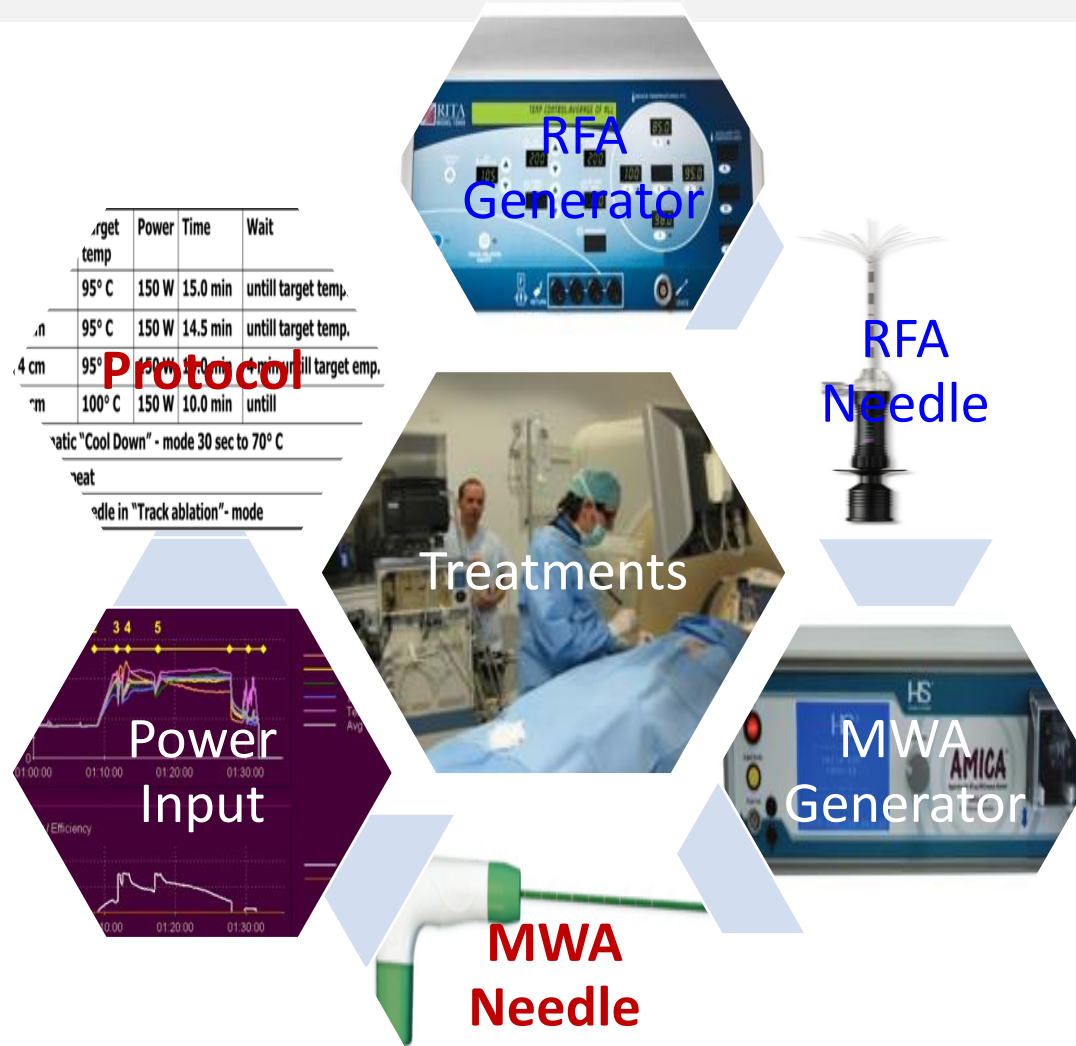
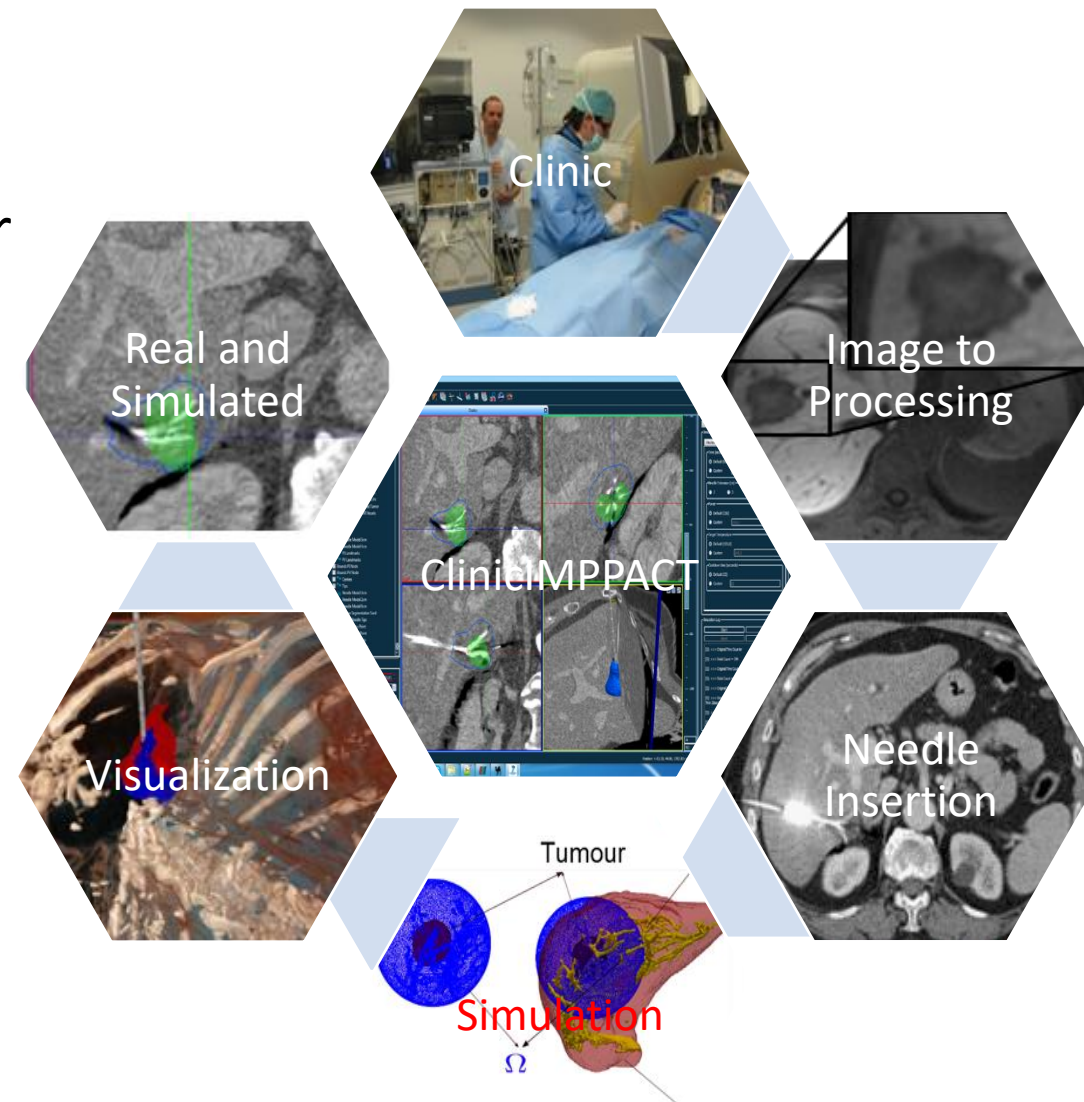


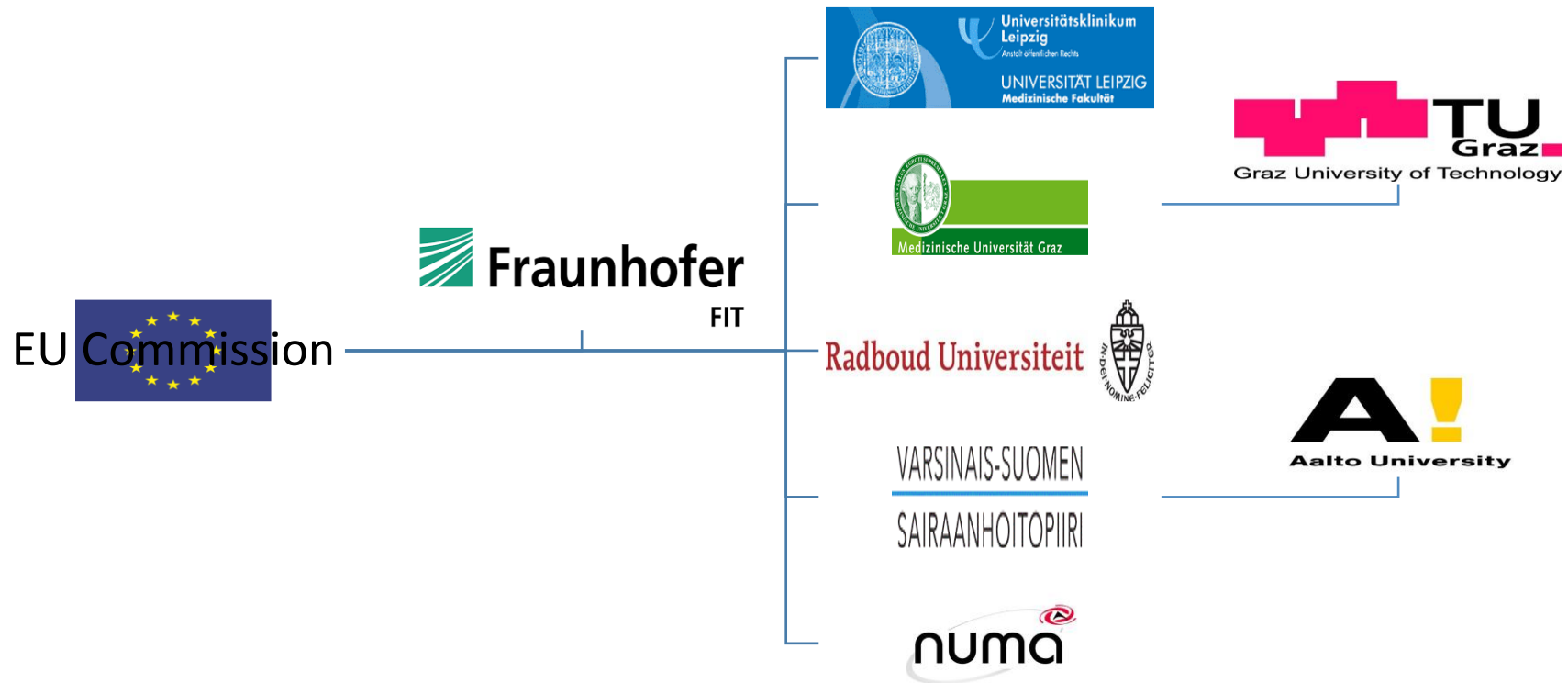
Image Sources: <https://angiodynamics.com>
<https://http://www.mermaidmedical.dk/>

- 🔗 Developed a software tool such that
 - Useful for the RFA treatment of liver cancer
 - Runs on a Single-PC
 - Usable at clinical environment
 - Predicts the lesion on the day of the treatment within few seconds
 - Accepts Patient-Specific parameters
 - Accepts Device-Specific parameters
 - Cost-efficient



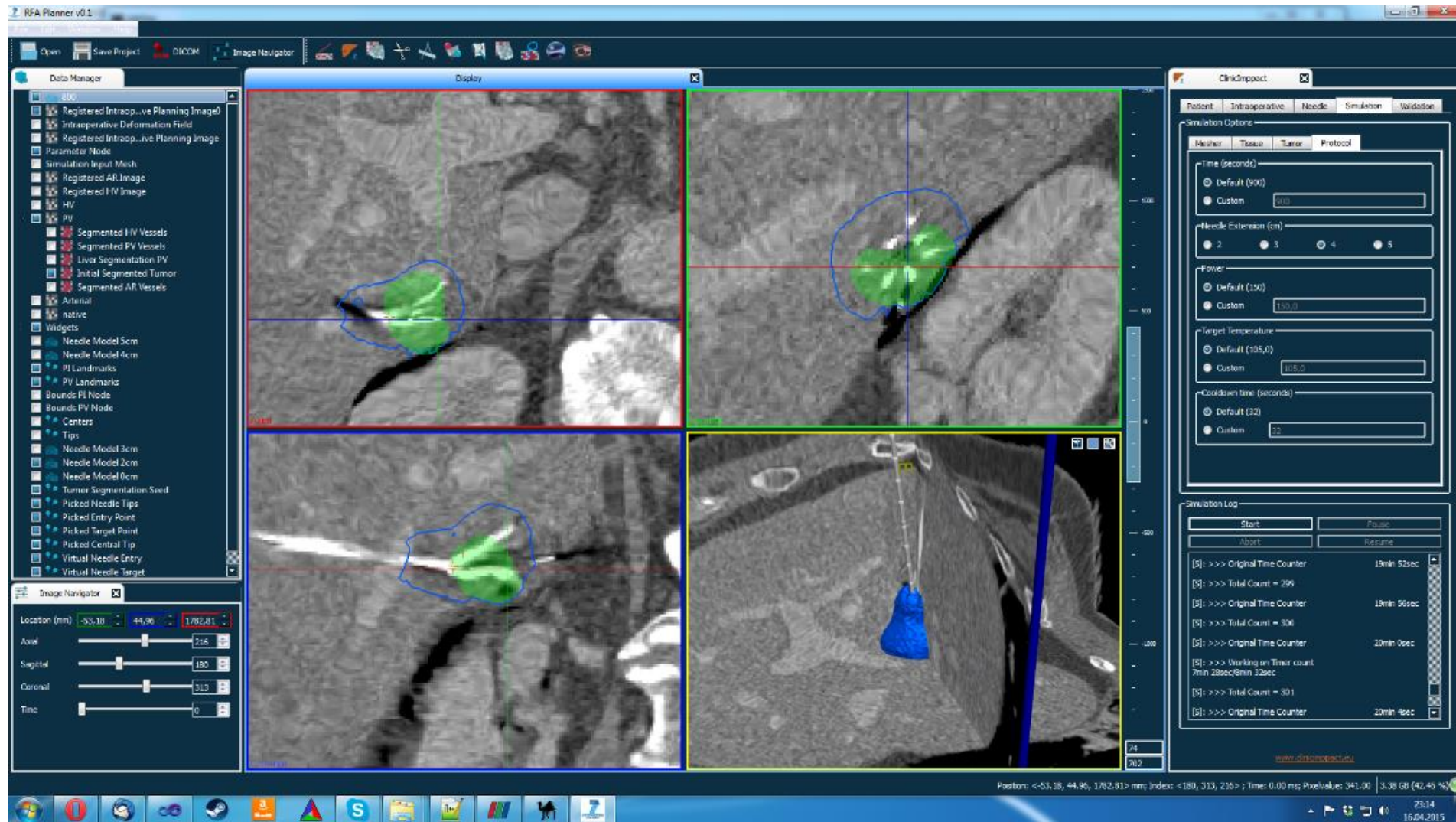
ClinicIMPACT Project

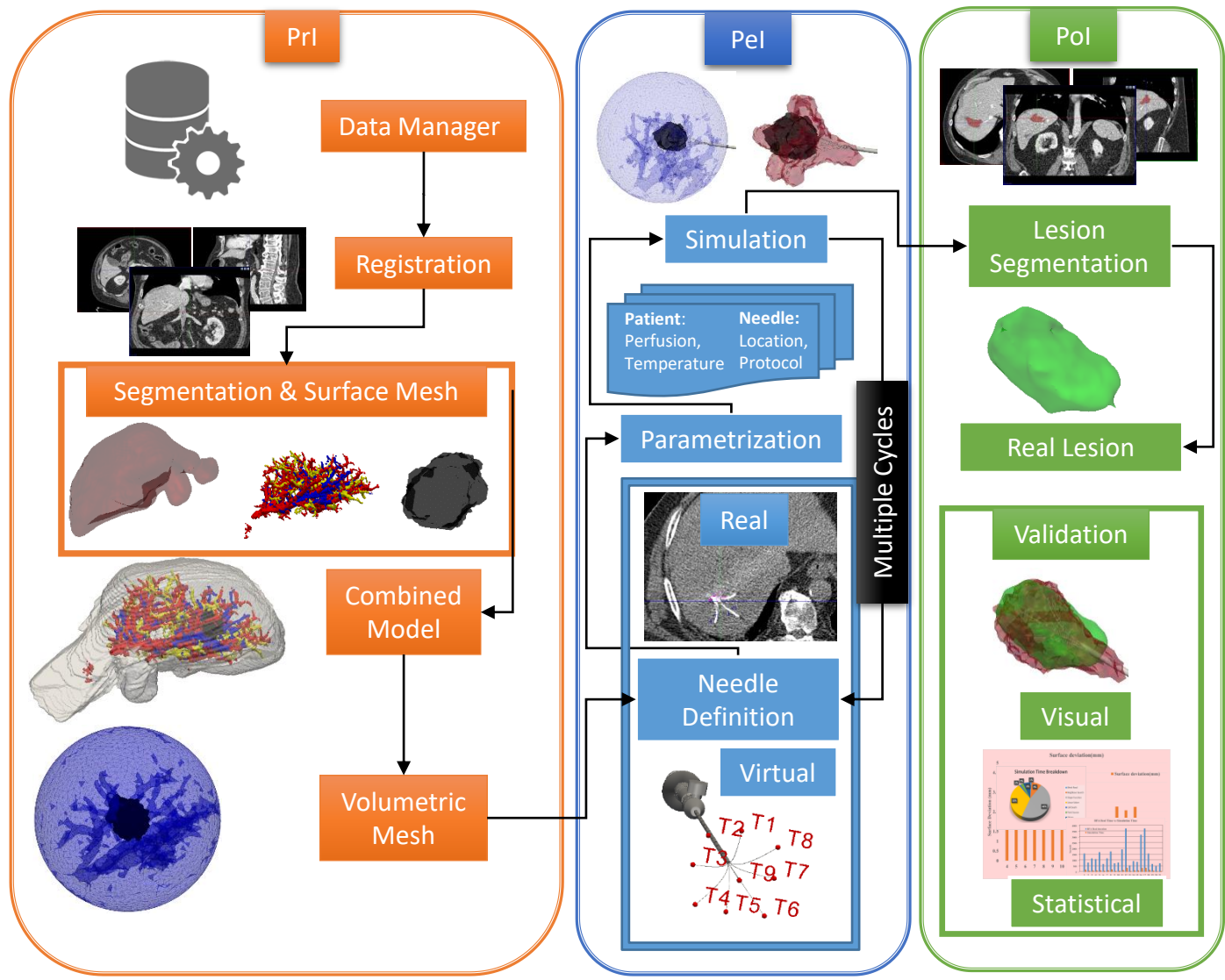
Clinical Intervention Modelling, Planning and Proof for Ablation Cancer Treatment



Rs.~41 Crores

<http://www.clinicimpact.eu>



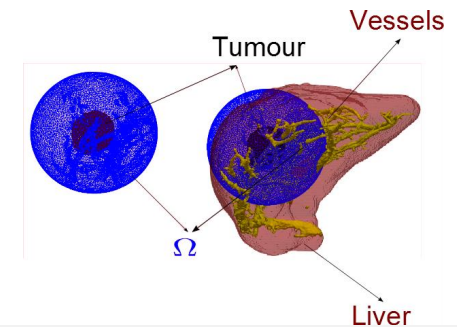


Bioheat Equation¹

$$\rho C \frac{\partial T}{\partial t} = k \Delta T + \omega_b \rho_b C_b (T_a - T) + Q_r \text{ on } \Omega$$

$$h_c T + k \frac{\partial T}{\partial \vec{n}} = h_c T_\infty \text{ on vessels boundary}$$

$$T = T_0 \text{ on } \partial\Omega$$



Cell Death Model²

$$\frac{dA}{dt} = -k_f e^{\frac{T}{T_k}} (1 - A)A + k_b (1 - A - D)$$

$$\frac{dD}{dt} = k_f e^{\frac{T}{T_k}} (1 - A) (1 - A - D)$$

$$A(0) = 0.99, D(0) = 0.0$$

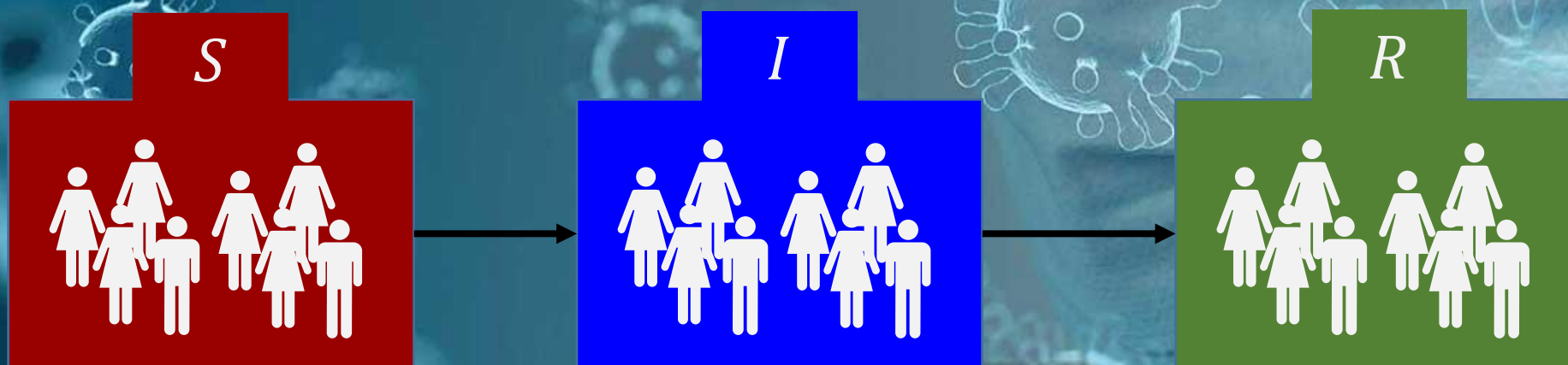
1. H. H. Pennes, Analysis of tissue and arterial blood temperature in the resting human forearm, J. Appl. Physio. 85(1):93-102, 1948
2. O'Neill DP, Peng T et al (2011) A three-state mathematical model of hyperthermic cell death. Ann Biomed Eng 39(1):570-579

SIR Model for COVID-19

Panchatcharam Mariappan

Associate Professor

**Department of Mathematics and Statistics,
IIT Tirupati**



COVID-2019

Simple Example

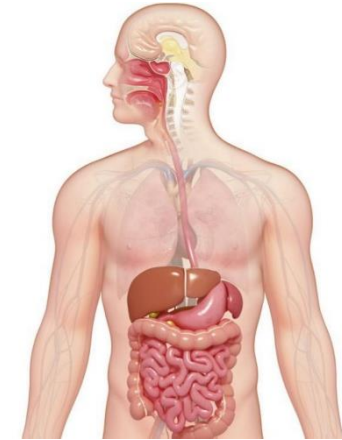
S



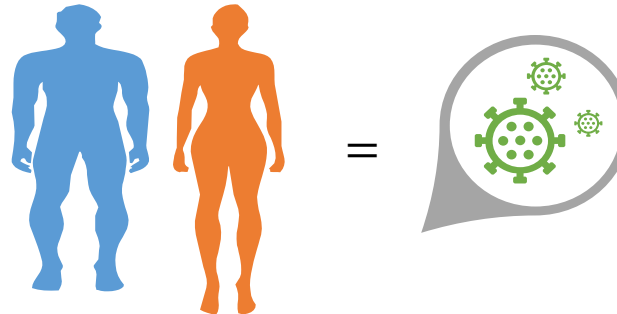
I



R

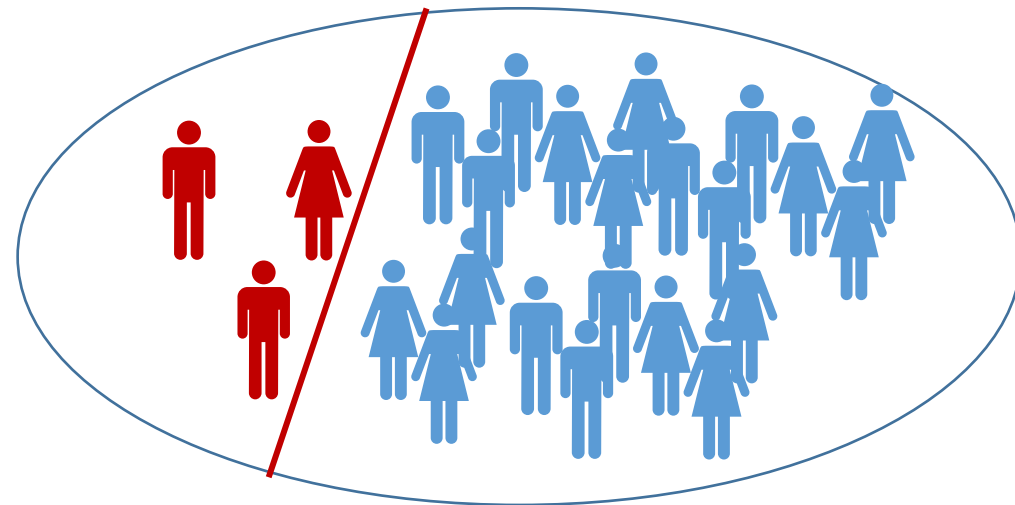


rice from the **S**ack taken
In the cooker, cooked and
Reached my mouth



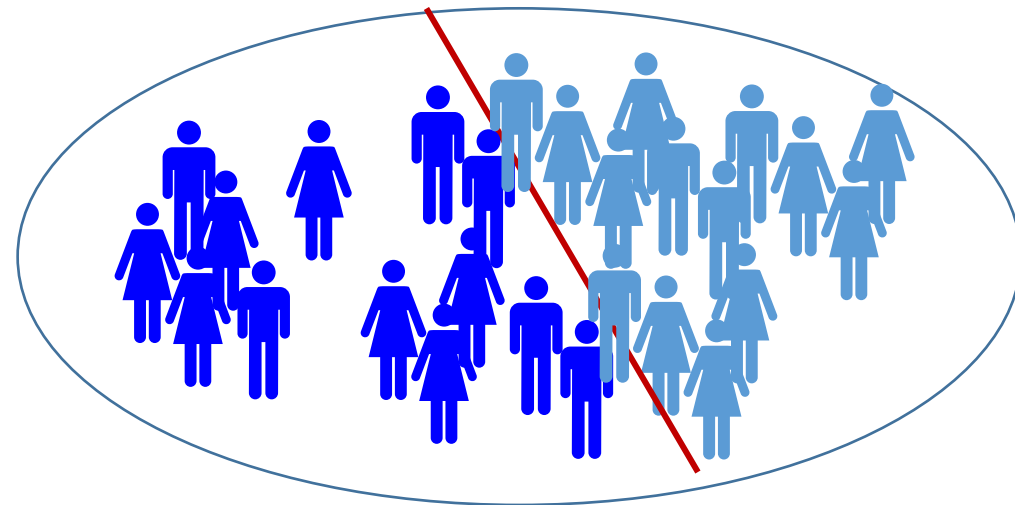
The class of individuals who are healthy but can contract the disease.

Denoted by S



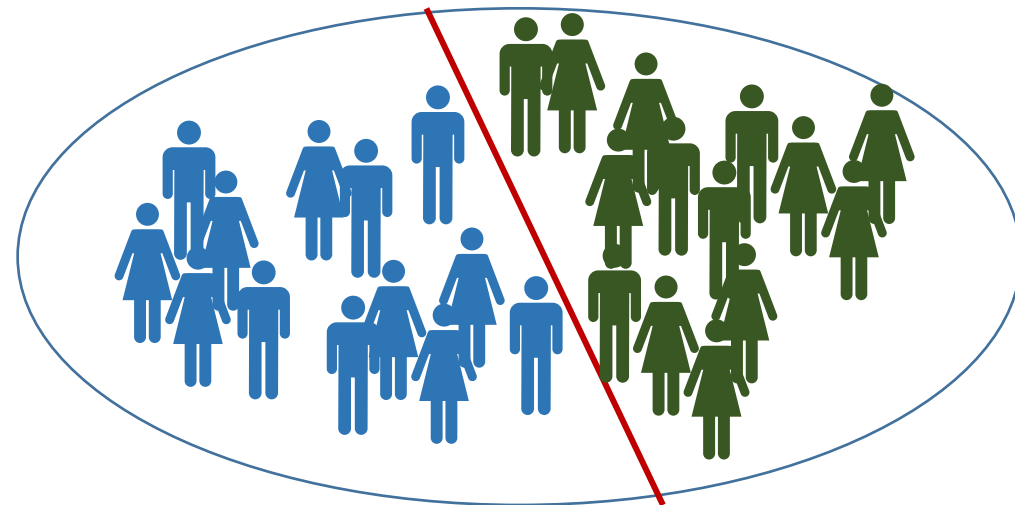
The class of individuals who have contracted the disease and are now sick with it.

Denoted by I



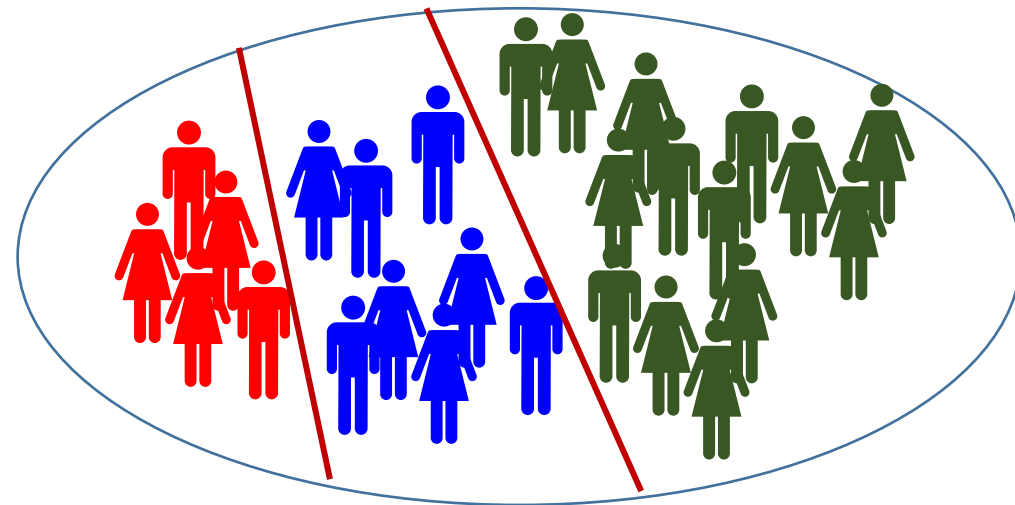
The class of individuals who have recovered and cannot contract the disease again.

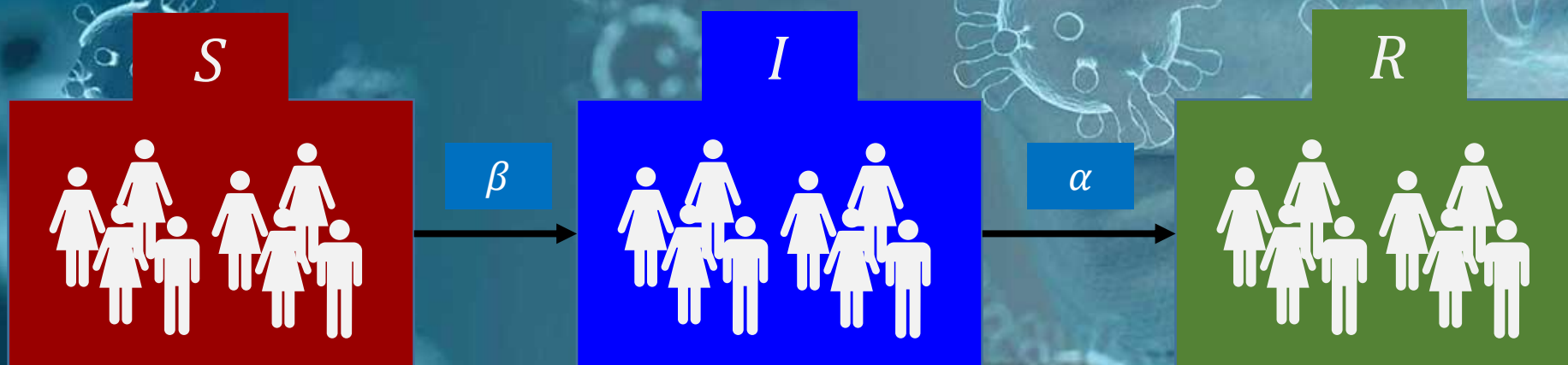
Denoted by R



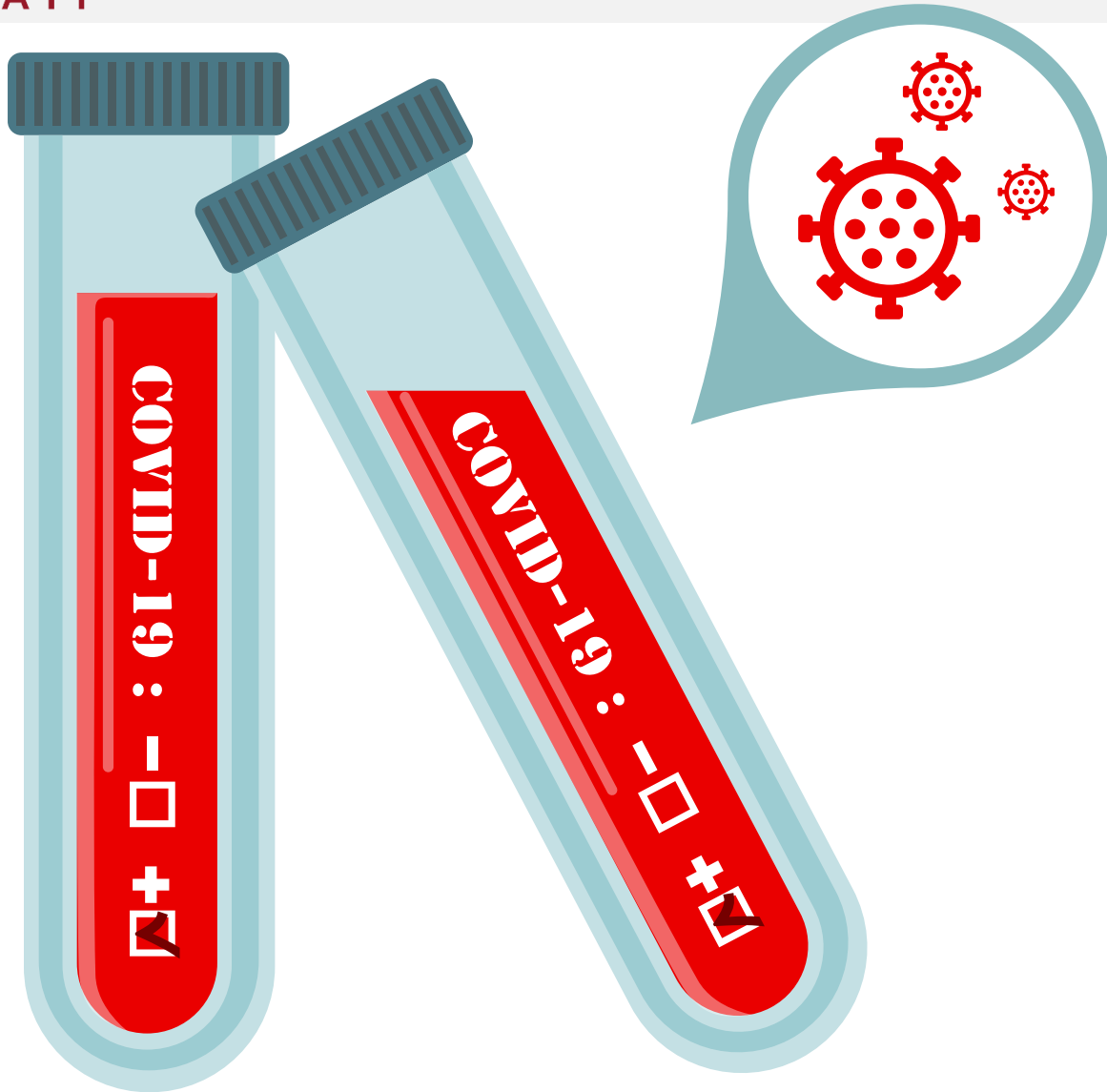
The total population size is the sum of susceptible, infectious and recovered

Denoted by N





COVID-2019



SIR Model

2019-2020

COVID-19

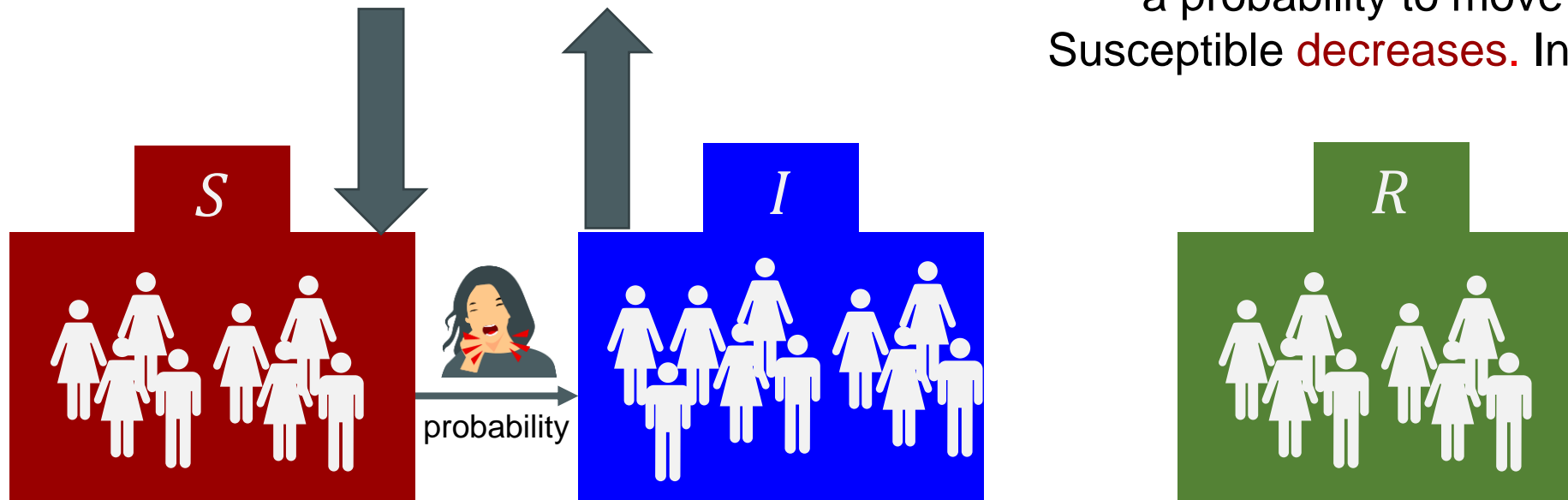
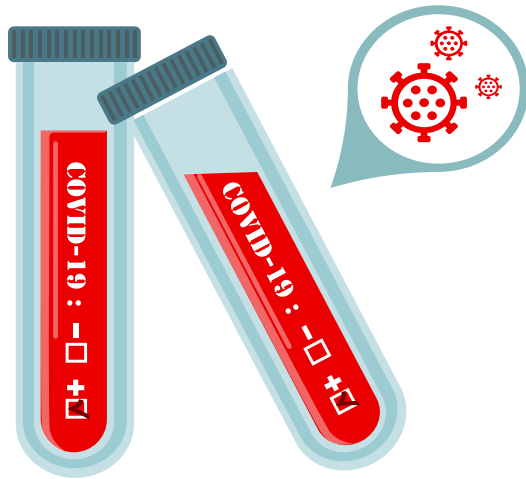
Assumptions

We assume the following
Infected individual becomes infectious
Total Population size is constant

COVID-19

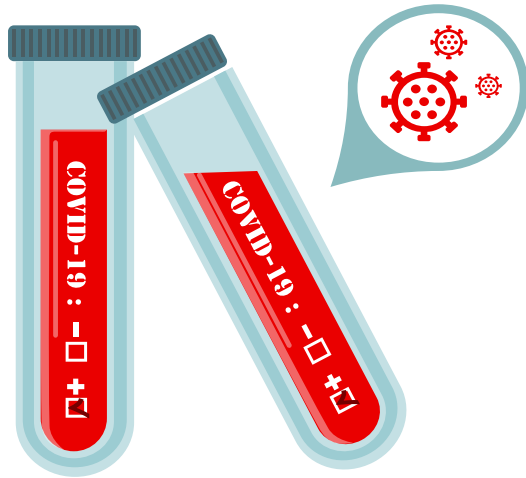
Differential Equation

Observe how the classes change over time.
When a susceptible contact with infectious, there is
a probability to move to infected class
Susceptible **decreases**. Infected **increases**



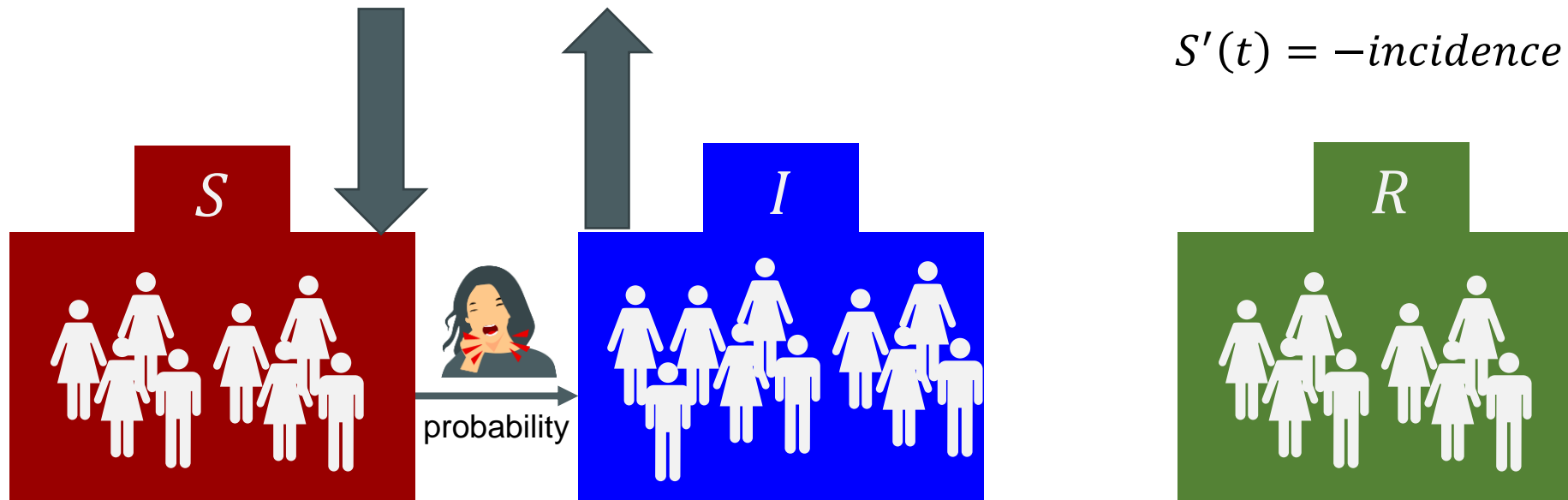
COVID-19

Differential Equation



Incidence
The number of individuals who become infected per unit of time

$$S'(t) = -incidence$$

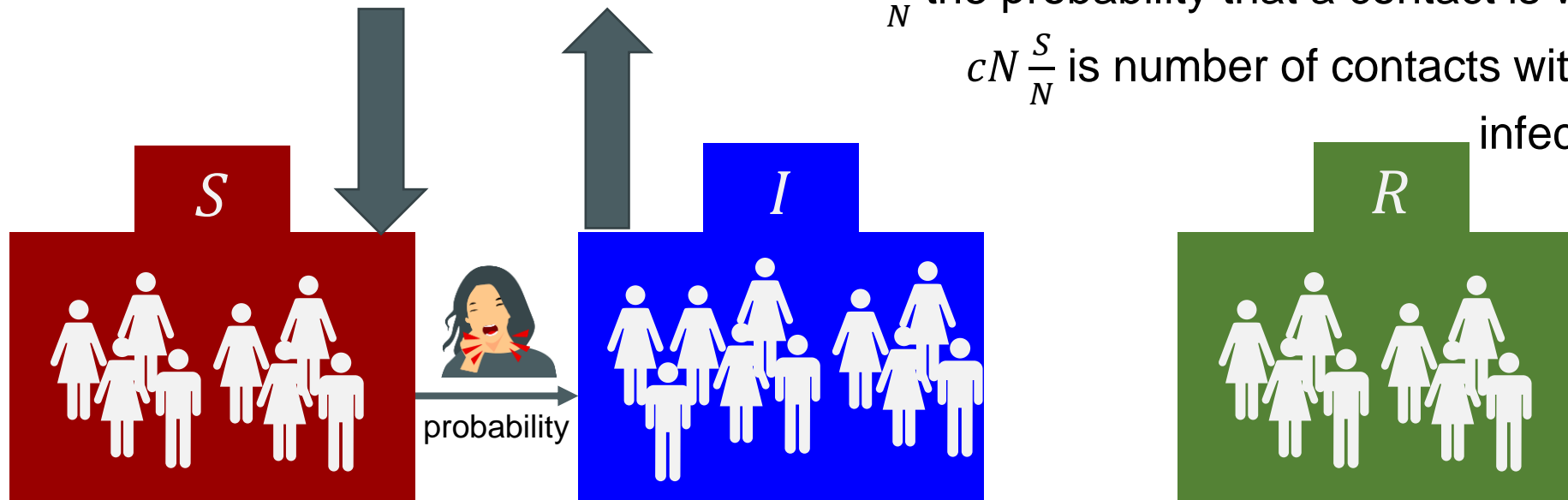
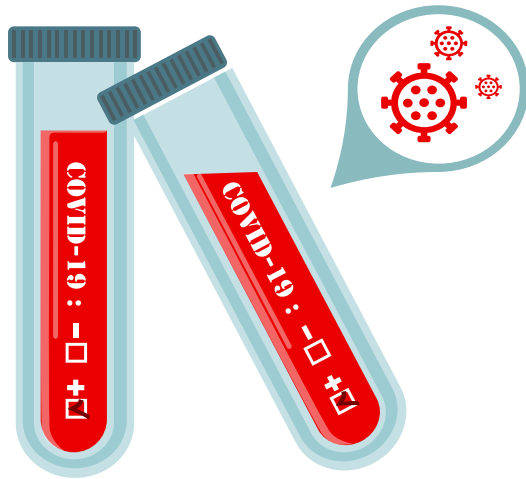


COVID-19

Differential Equation

Incidence

Let cN denote the number of contacts per unit time infected contacts. Where c denotes per capita rate $\frac{S}{N}$ the probability that a contact is with a susceptible $cN \frac{S}{N}$ is number of contacts with susceptible per infected per unit time.



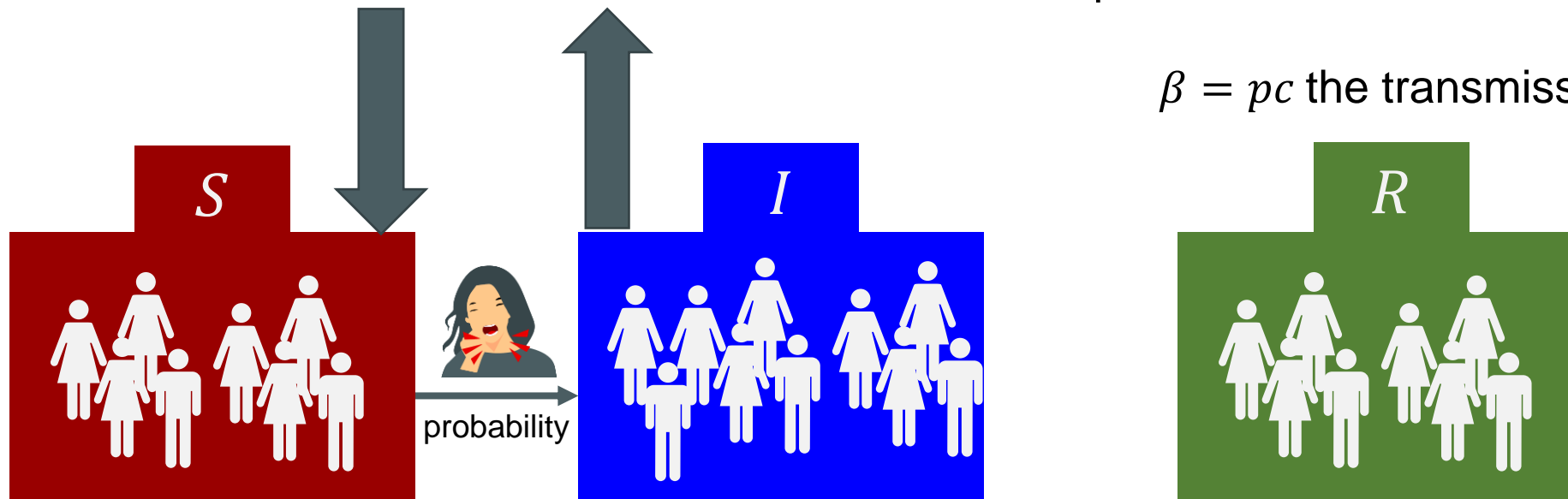
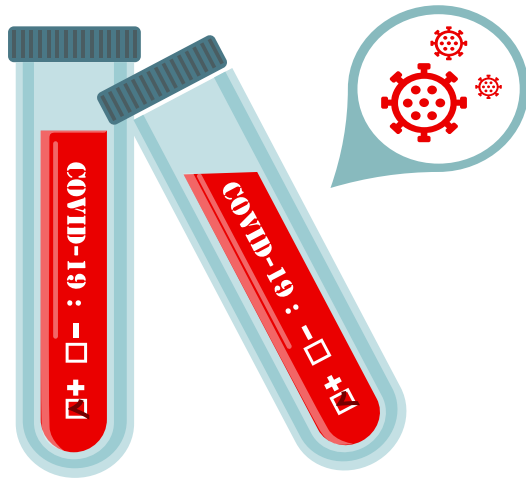
COVID-19

Differential Equation

Incidence

If p is the probability that a contact with a susceptible results in transmission, then pcS is the number of susceptible moves to infected per unit time per infected persons.

$\beta = pc$ the transmission rate constant



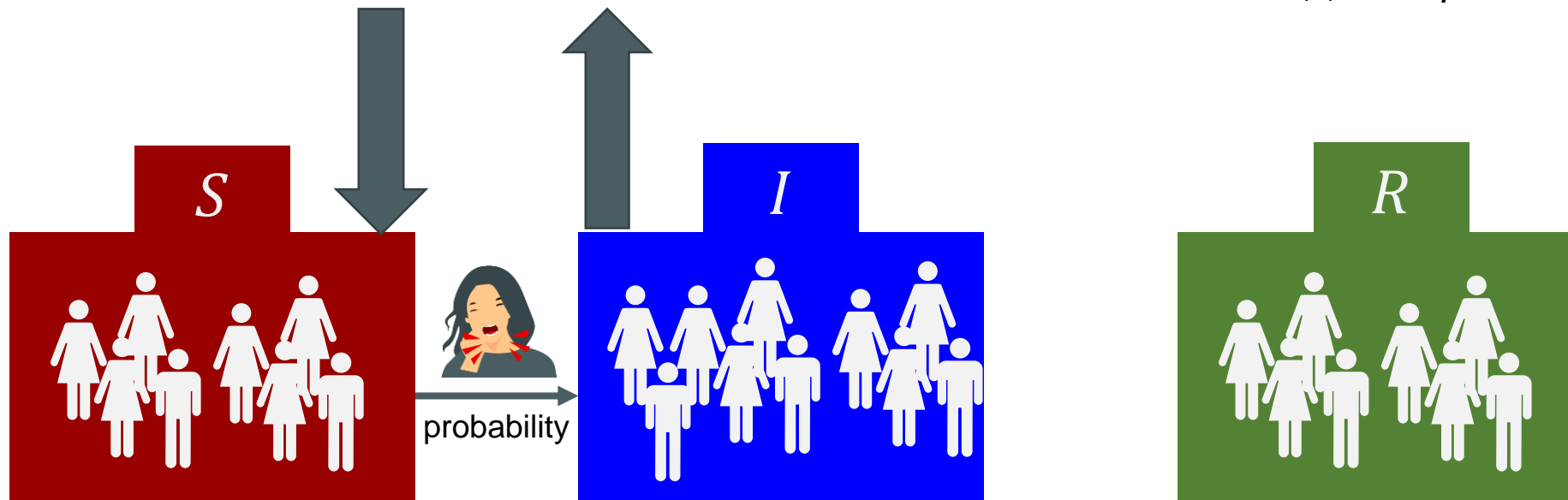
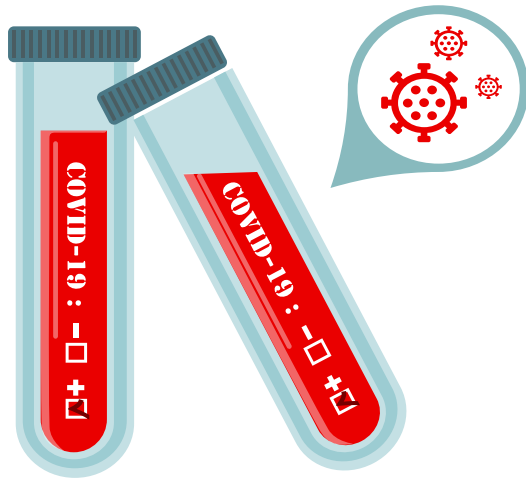
COVID-19

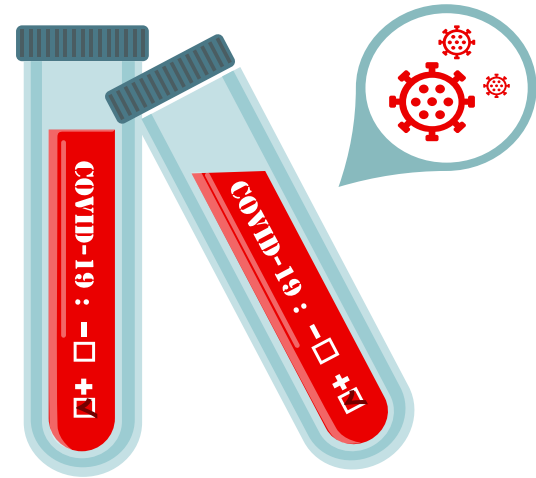
Differential Equation

Incidence

βSI denote the number of people who become infected per unit time = incidence

$$S'(t) = -\beta SI$$



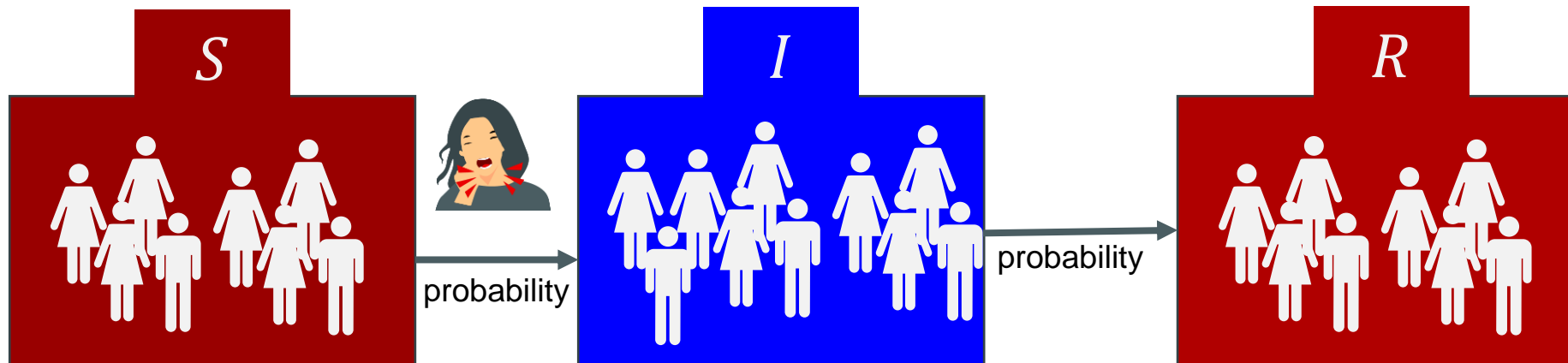


COVID-19

Differential Equation

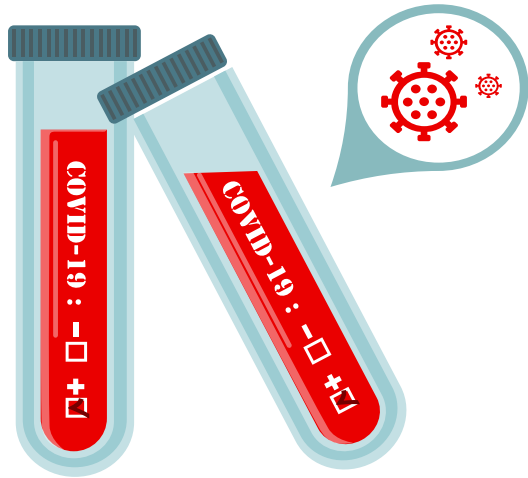
Recovery Rate

Similarly, infected may move to recovery or removed class at a constant rate per capita probability per unit time α



COVID-19

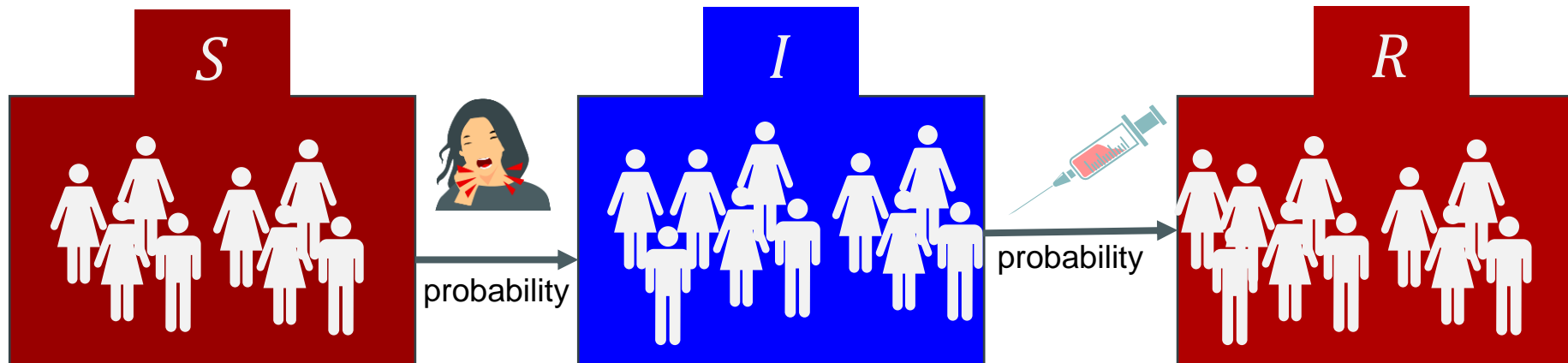
Differential Equation



Recovery Rate

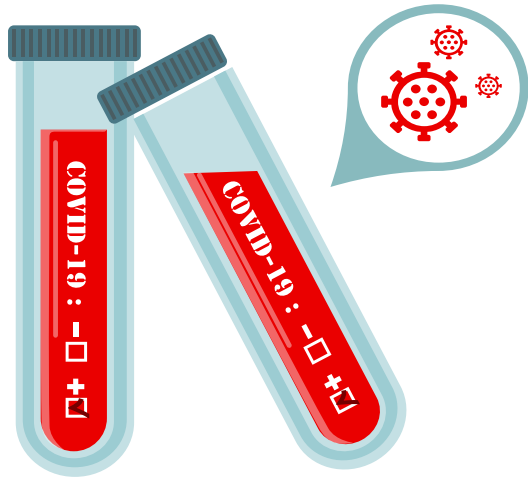
αI is the number of infected moved to recover/remove
Since from susceptible, βIS moved to infected and αI
moved from infected to recovered, we have

$$I'(t) = \beta IS - \alpha I$$



COVID-19

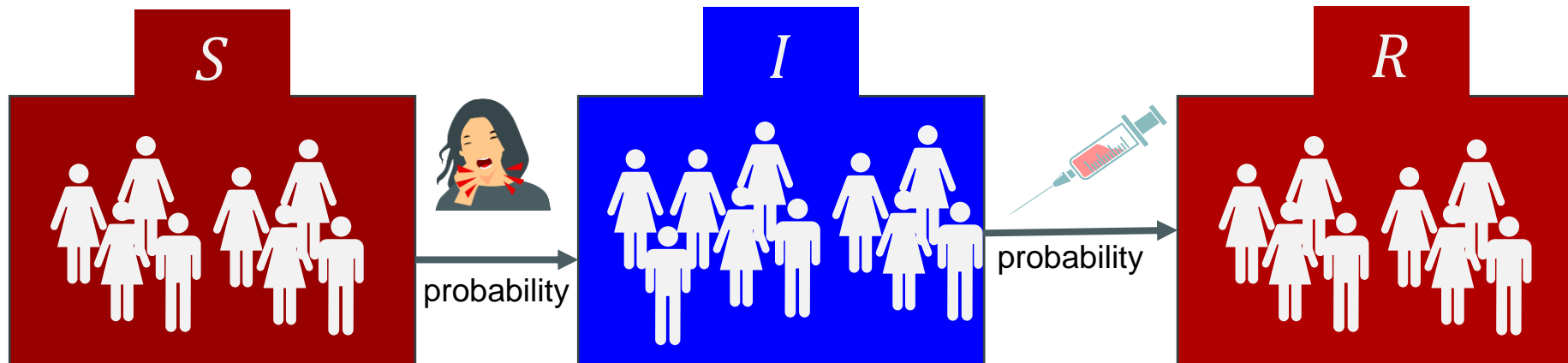
Differential Equation



Recovery Rate

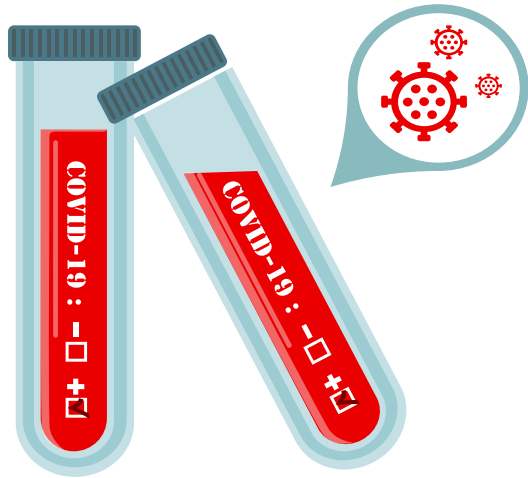
Recovered persons move from infected to recover class is given by

$$R'(t) = \alpha I$$

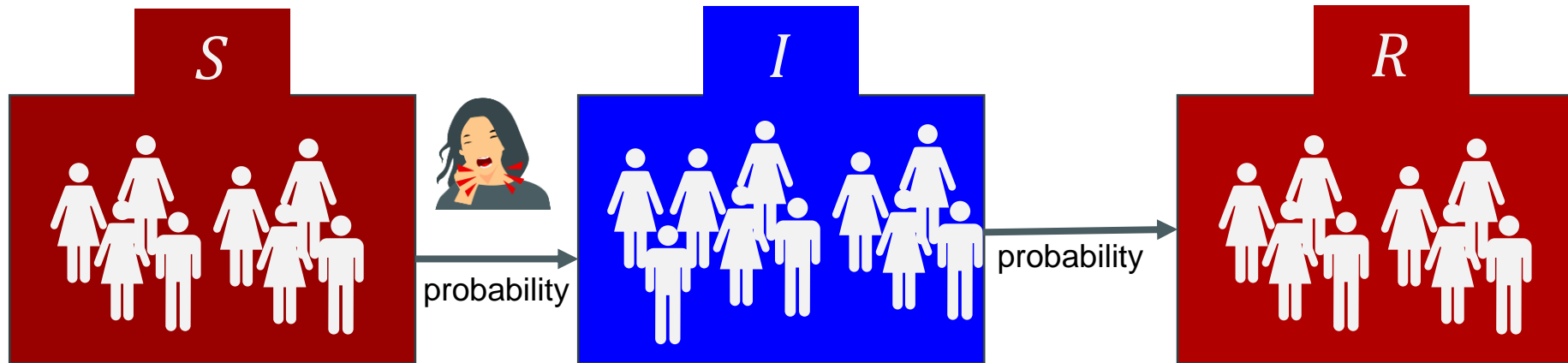


COVID-19

SIR Model



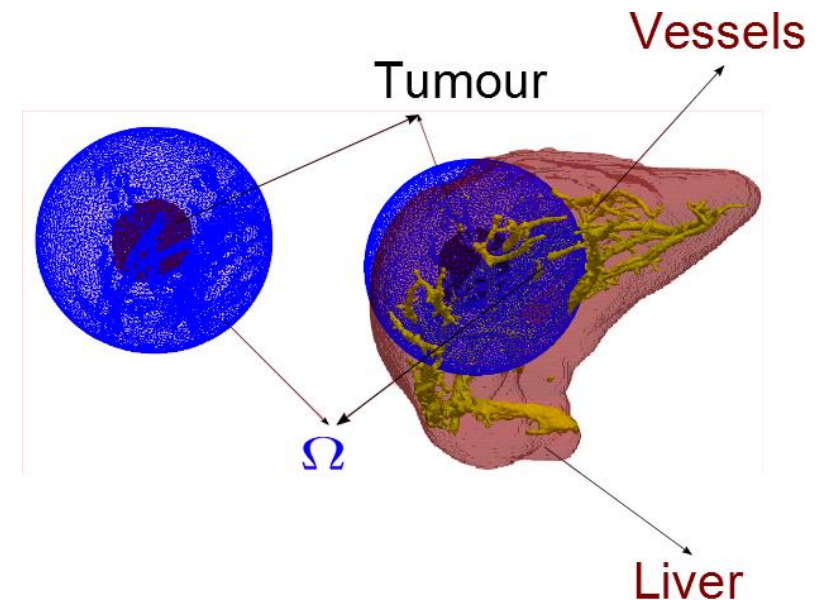
$$\begin{aligned}S'(t) &= -\beta IS \\I'(t) &= \beta IS - \alpha I \\R'(t) &= \alpha I \\S(0), I(0), R(0) \\N &= S(0) + I(0) + R(0)\end{aligned}$$



$$\rho C \frac{\partial T}{\partial t} = k \Delta T + \omega_b \rho_b C_b (T_a - T) + Q_r \text{ on } \Omega$$

$$h_c T + k \frac{\partial T}{\partial \vec{n}} = h_c T_\infty \text{ on vessels boundary}$$

$$T = T_0 \text{ on } \partial\Omega$$



1. H. H. Pennes, Analysis of tissue and arterial blood temperature in the resting human forearm, J. Appl. Physio. 85(1):93-102, 1948

Cell Death Model

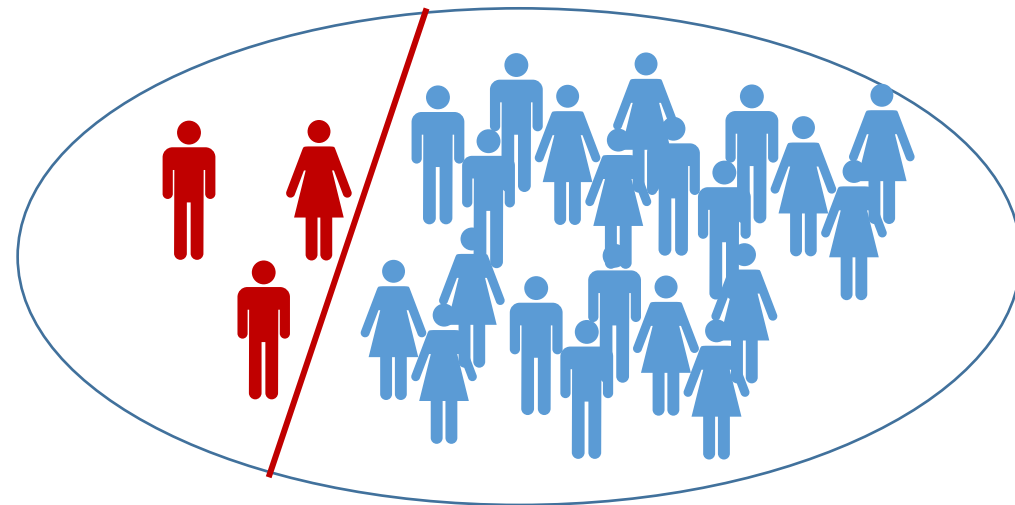
Panchatcharam Mariappan

Associate Professor

**Department of Mathematics and Statistics,
IIT Tirupati**

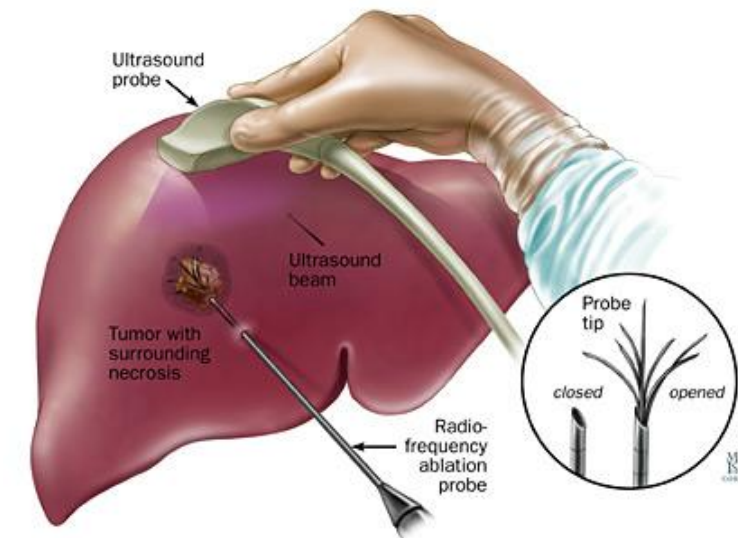
The class of individuals who are healthy but can contract the disease.

Denoted by S



- Area of coagulative necrosis created by the RFA procedure
- Region covered by dead and damaged cells due to heat

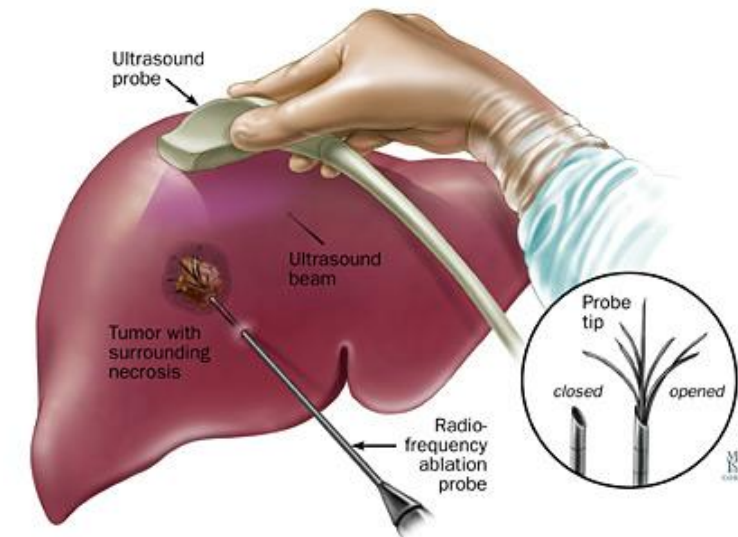
Success of the RFA is decided by the ablation zone



- Cell damage occurs when temperature rises above 43°C
 - Temperature and Heating time plays vital role

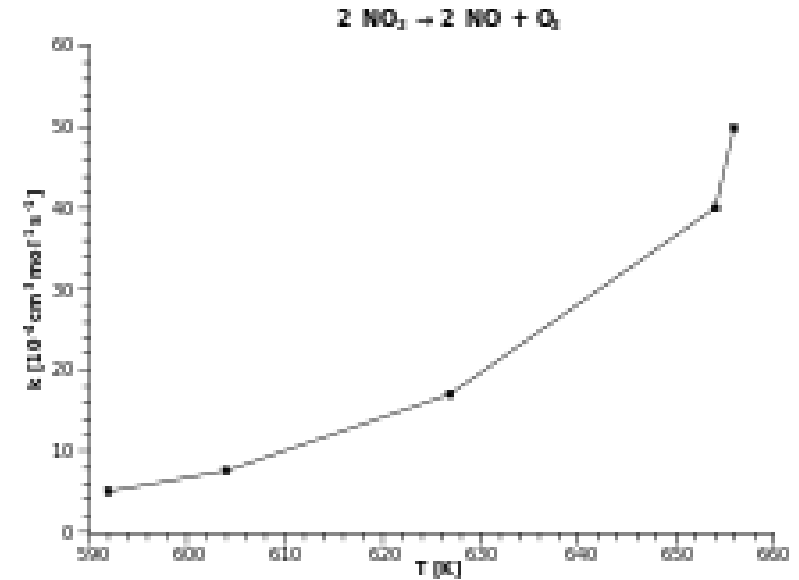
Simplest model:

- Single temperature threshold ($50^{\circ}\text{C} - 60^{\circ}\text{C}$)
 - Below threshold active cells
 - Above threshold dead cells



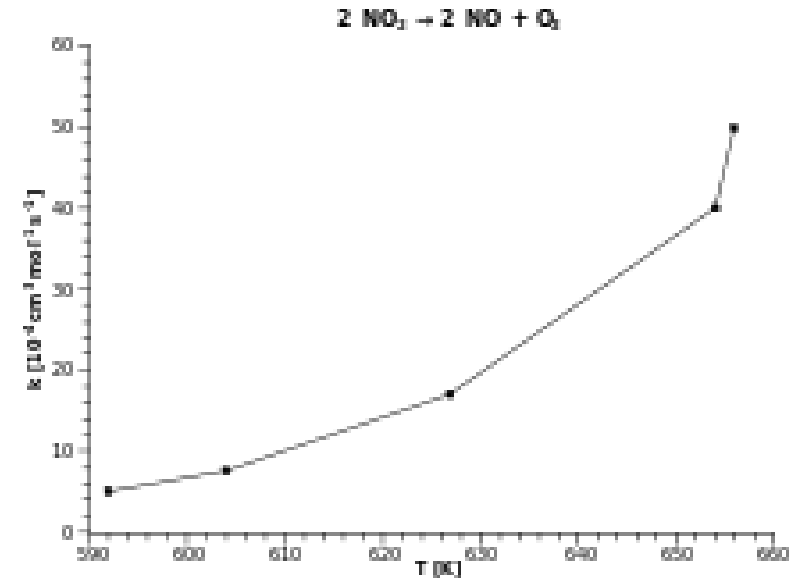
$$k = Ae^{-\frac{E_a}{RT}}$$

- E_a : activation energy
- T : temperature
- R : universal constant
- A : exponential factor

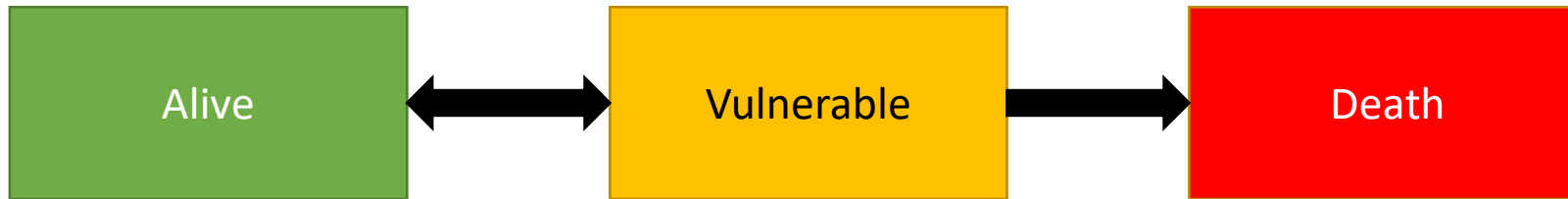


$$\Omega(t) = \int_0^{\tau} A \exp\left(-\frac{E_a}{RT(t)}\right) dt$$

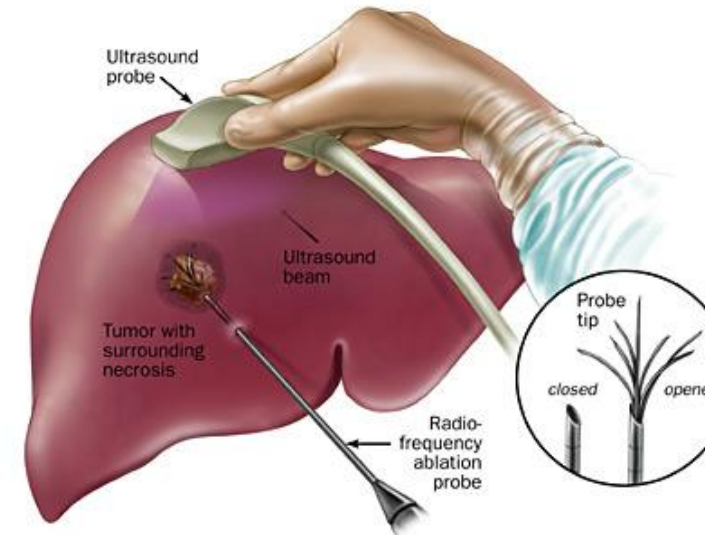
- E_a : activation energy
- T : temperature
- R : universal constant
- A : exponential factor



Cell Death Model



1. O'Neill DP, Peng T et al (2011) A three-state mathematical model of hyperthermic cell death. *Ann Biomed Eng* 39(1):570-579



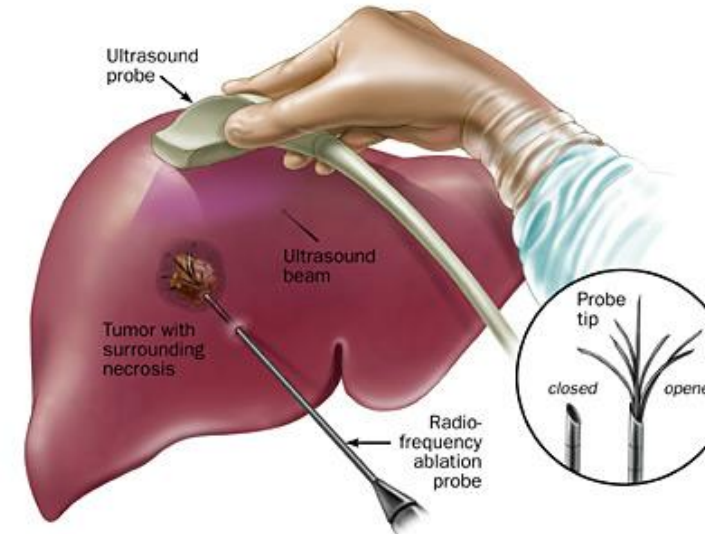
Cell Death Model

$$\frac{dA}{dt} = -k_f e^{\frac{T}{T_k}} (1 - A)A + k_b (1 - A - D)$$

$$\frac{dD}{dt} = k_f e^{\frac{T}{T_k}} (1 - A) (1 - A - D)$$

$$A(0) = 0.99, D(0) = 0.0$$

1. O'Neill DP, Peng T et al (2011) A three-state mathematical model of hyperthermic cell death. Ann Biomed Eng 39(1):570-579



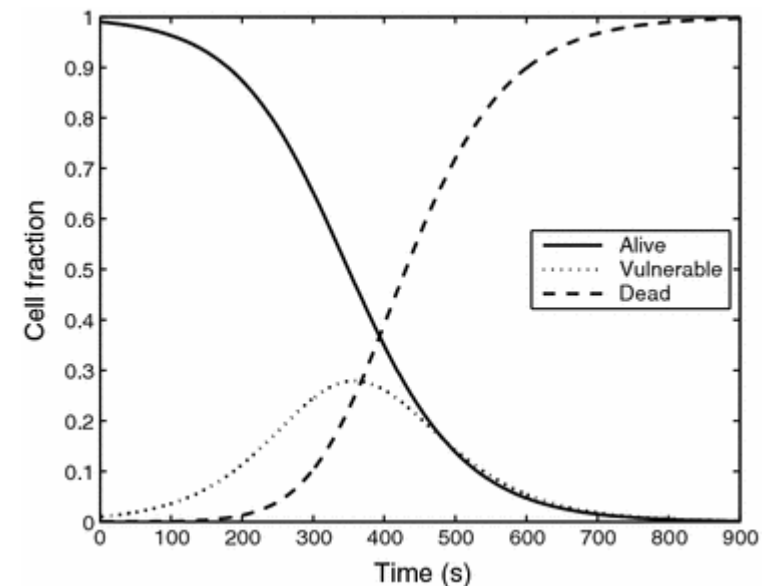
Cell Death Model

$$\frac{dA}{dt} = -k_f e^{\frac{T}{T_k}} (1 - A)A + k_b (1 - A - D)$$

$$\frac{dD}{dt} = k_f e^{\frac{T}{T_k}} (1 - A) (1 - A - D)$$

$$A(0) = 0.99, D(0) = 0.0$$

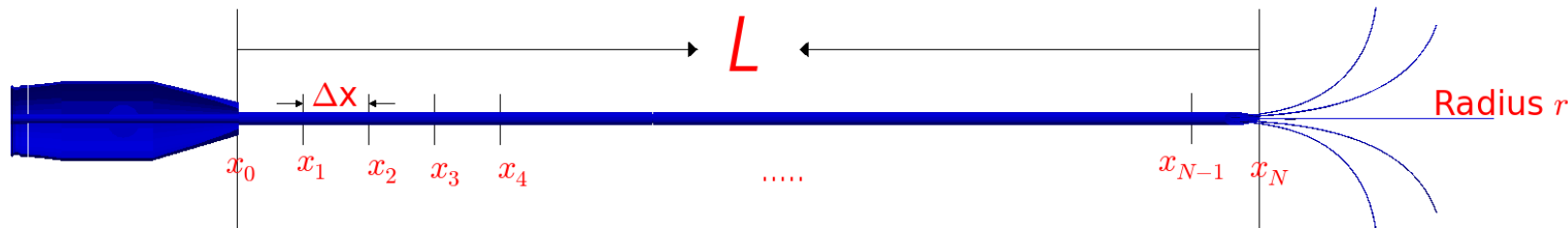
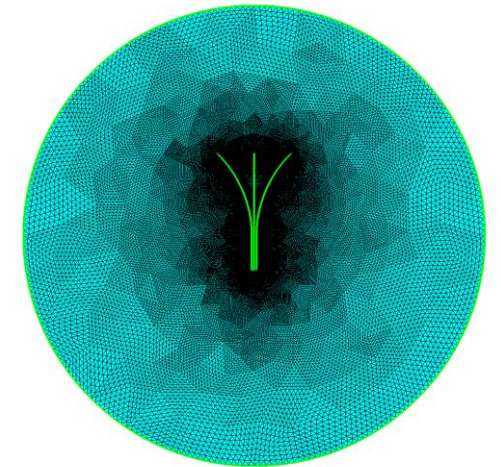
1. O'Neill DP, Peng T et al (2011) A three-state mathematical model of hyperthermic cell death. Ann Biomed Eng 39(1):570-579



$$\sigma \Delta \phi = 0 \text{ on } \Omega$$

$$\phi = \begin{cases} \phi_r & \text{on Needle Tips} \\ \phi_c & \text{on Circular boundary} \end{cases}$$

$$\frac{\partial \phi}{\partial n} = 0 \text{ on Needle Shaft}$$



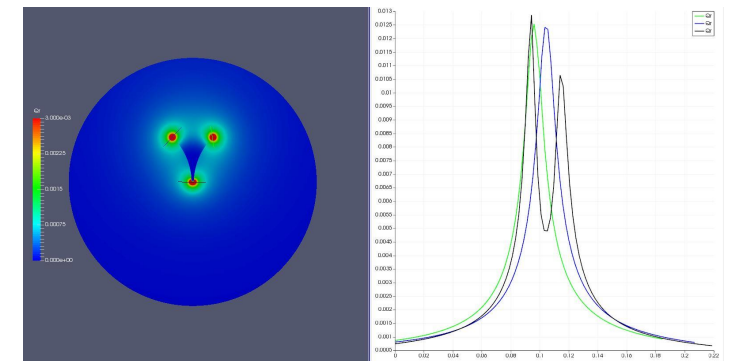
$$Q_r = \sigma |\nabla \phi|^2$$

Gaussian:

$$P(\vec{x}) = \frac{\sum_{tip} \alpha_{tip} \exp\left(-\frac{\|\vec{x} - \vec{x}_{tip}\|^2}{2\sigma^2}\right)}{\sum_{tip} \alpha_{tip} (\sigma\sqrt{2\pi})^3}$$

Heat Source: $Q_r = \sum P(\vec{x}) * power$

Power Adjustment: PID Controller



Joule Heat/Point Source Model

Panchatcharam Mariappan

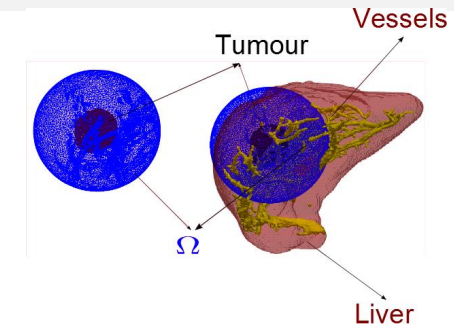
Associate Professor

**Department of Mathematics and Statistics,
IIT Tirupati**

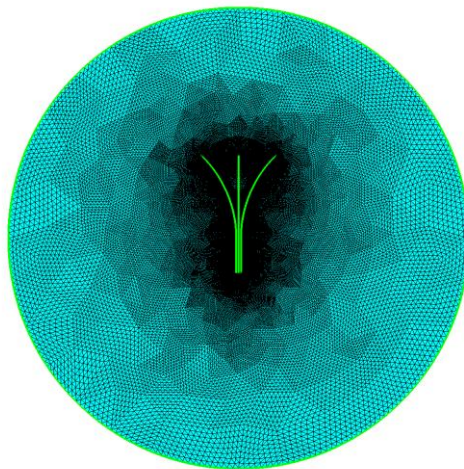
What is the Model?

Bioheat Equation¹

$$\rho C \frac{\partial T}{\partial t} = k \Delta T + \omega_b \rho_b C_b (T_a - T) + Q_r \text{ on } \Omega$$



Joule Heat Model



$$\sigma \Delta \phi = 0 \text{ on } \Omega$$

$$\phi = \begin{cases} \phi_r \text{ on NeedleTips} \\ \phi_c \text{ on Circularboundary} \end{cases}$$

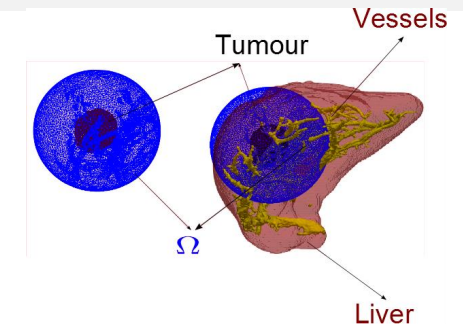
$$\frac{\partial \phi}{\partial n} = 0 \text{ on Needle shaft}$$

$$Q_r = \sigma (|\nabla \phi|^2)$$

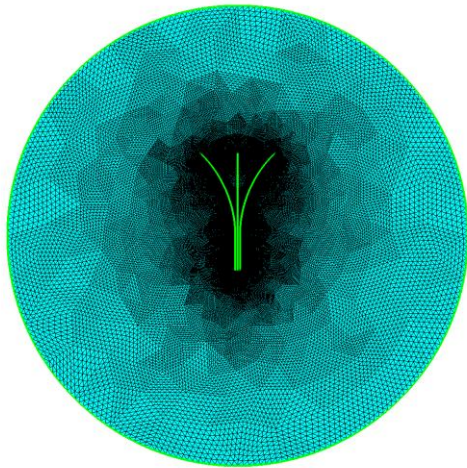
1. H. H. Pennes, Analysis of tissue and arterial blood temperature in the resting human forearm, J. Appl. Physio. 85(1):93-102, 1948
2. O'Neill DP, Peng T et al (2011) A three-state mathematical model of hyperthermic cell death. Ann Biomed Eng 39(1):570-579

Bioheat Equation¹

$$\rho C \frac{\partial T}{\partial t} = k \Delta T + \omega_b \rho_b C_b (T_a - T) + Q_r \text{ on } \Omega$$



Point Source Model



$$P(\vec{x}) = \frac{\sum_{tip} \alpha_{tip} \exp\left(-\frac{\|\vec{x} - \vec{x}_{tip}\|^2}{2\sigma^2}\right)}{\sum_{tip} \alpha_{tip} (\sigma\sqrt{2\pi})^3}$$

$$Q_r = \sum P(\vec{x}) * power$$

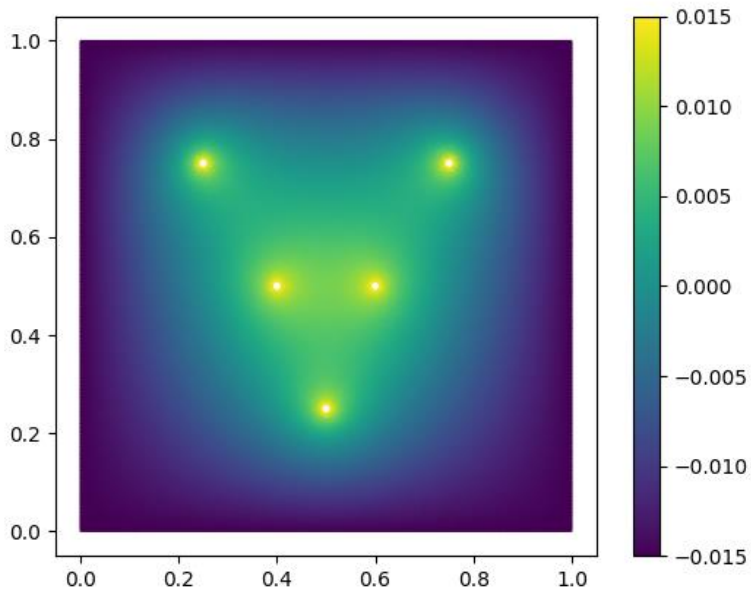
1. H. H. Pennes, Analysis of tissue and arterial blood temperature in the resting human forearm, J. Appl. Physio. 85(1):93-102, 1948
2. O'Neill DP, Peng T et al (2011) A three-state mathematical model of hyperthermic cell death. Ann Biomed Eng 39(1):570-579

How?

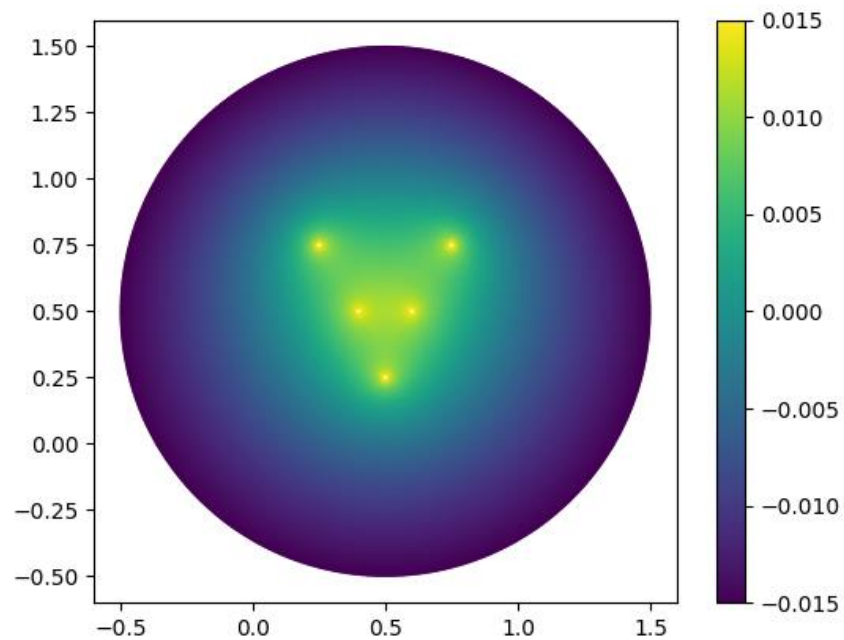
$$\varphi = \begin{cases} 0.015 & \text{on needle tips} \\ -0.015 & \text{on rectangular boundary} \end{cases}$$

$$\sigma = 0.4$$

Using FeniCS software



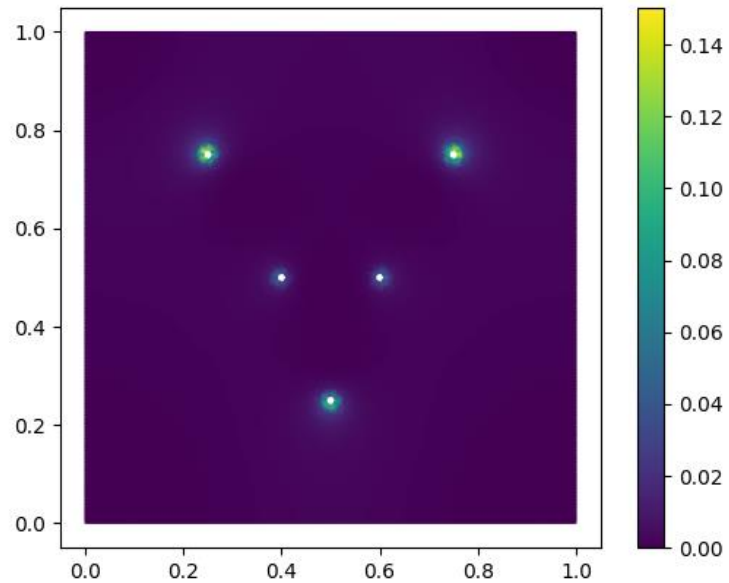
φ Visualization on unit square



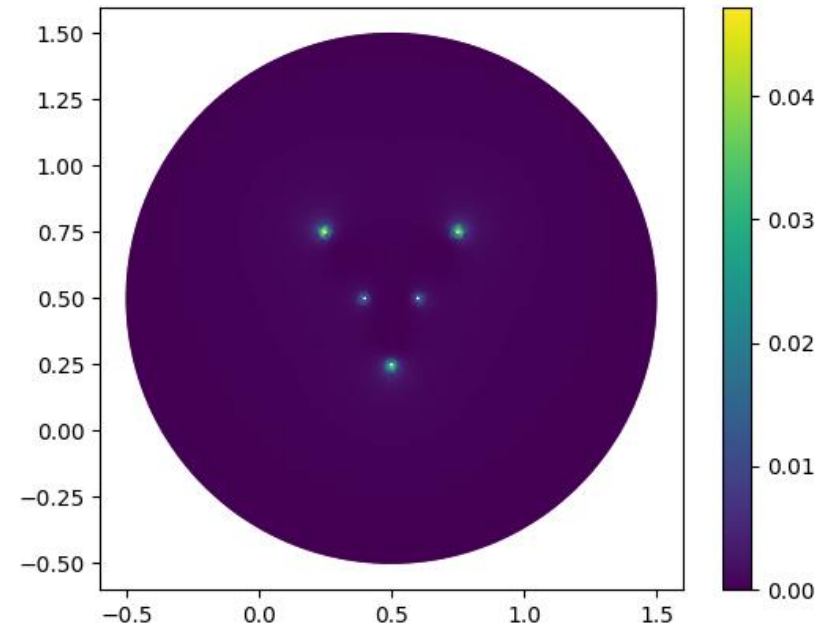
φ Visualization on circle

$$Q_r = \sigma(|\nabla\phi|^2) \quad \sigma = 0.4$$

Using FeniCS software

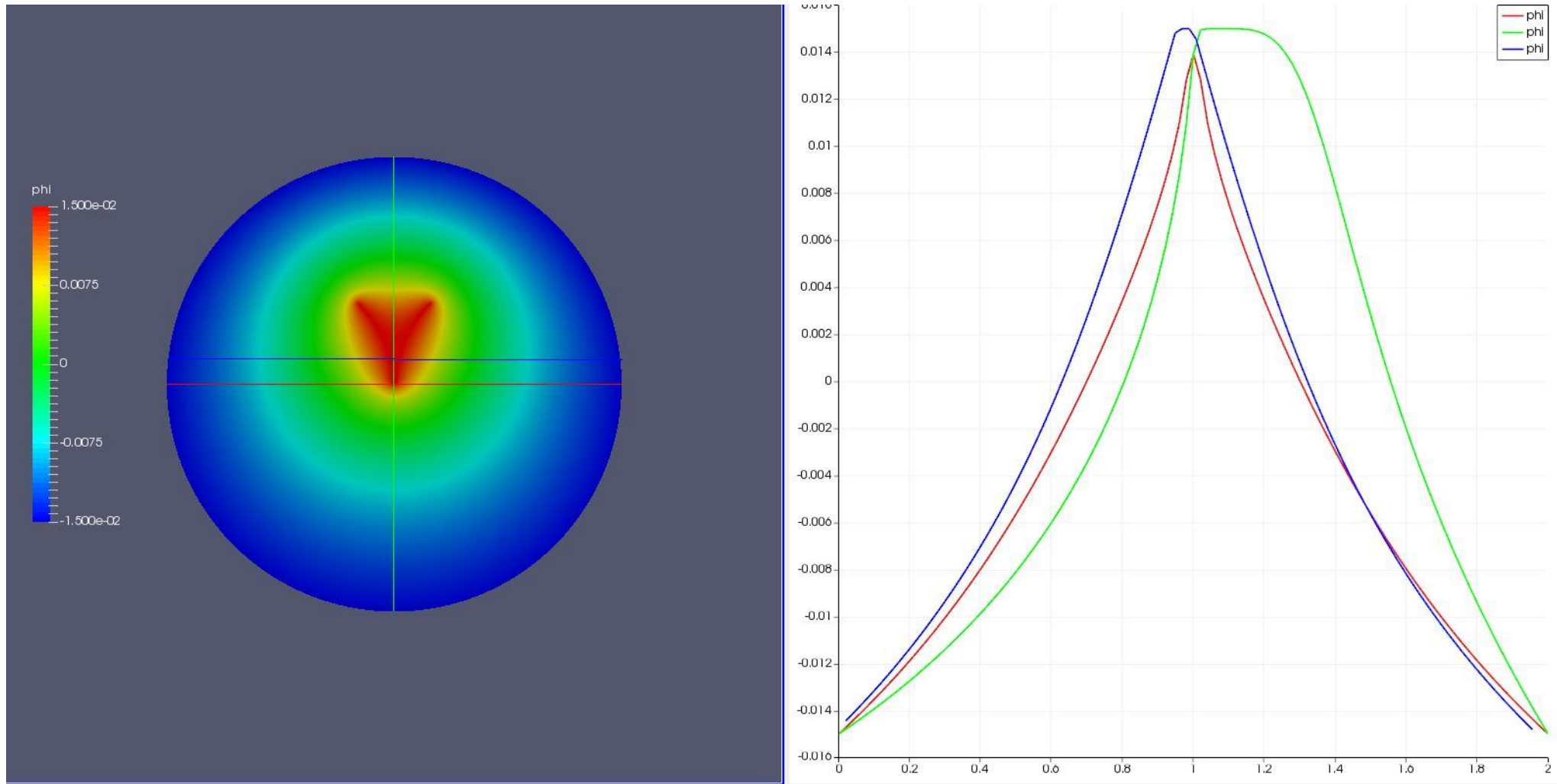


Q_r Visualization on unit square

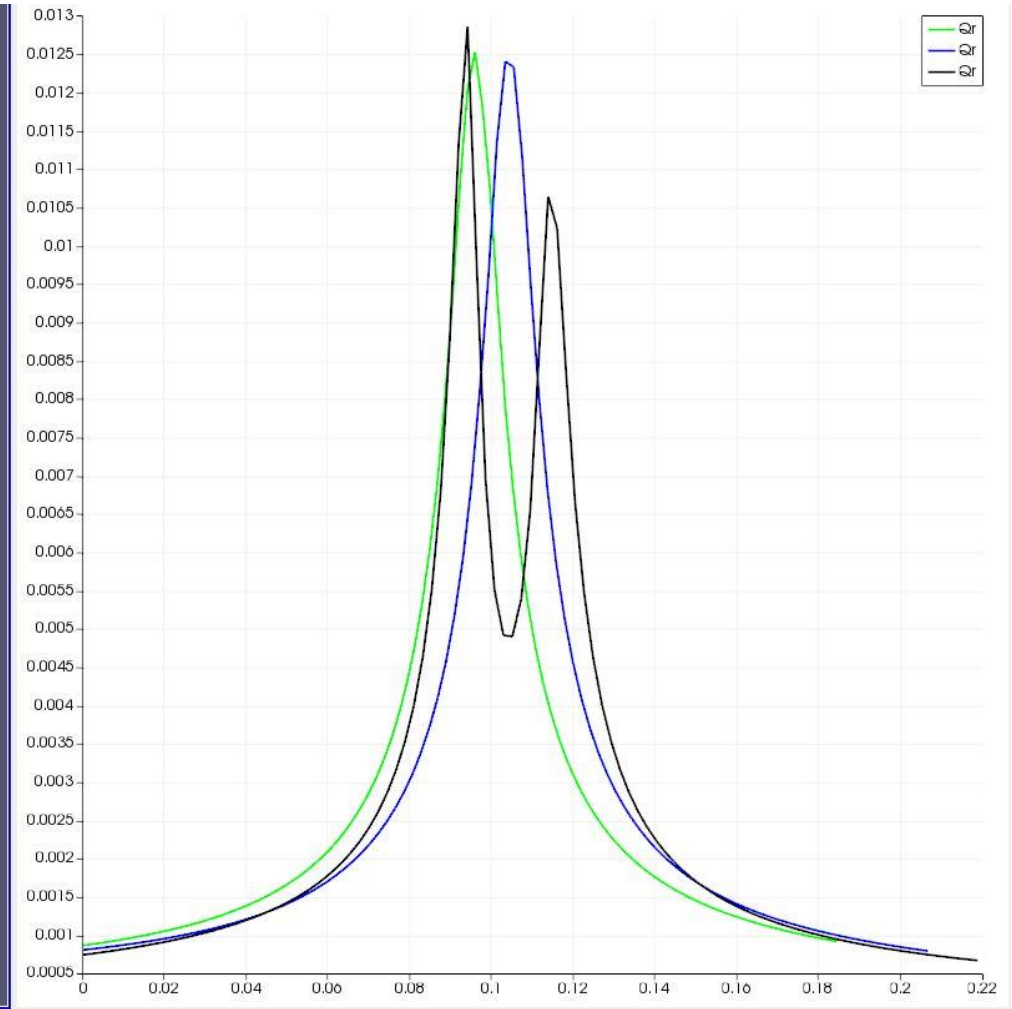
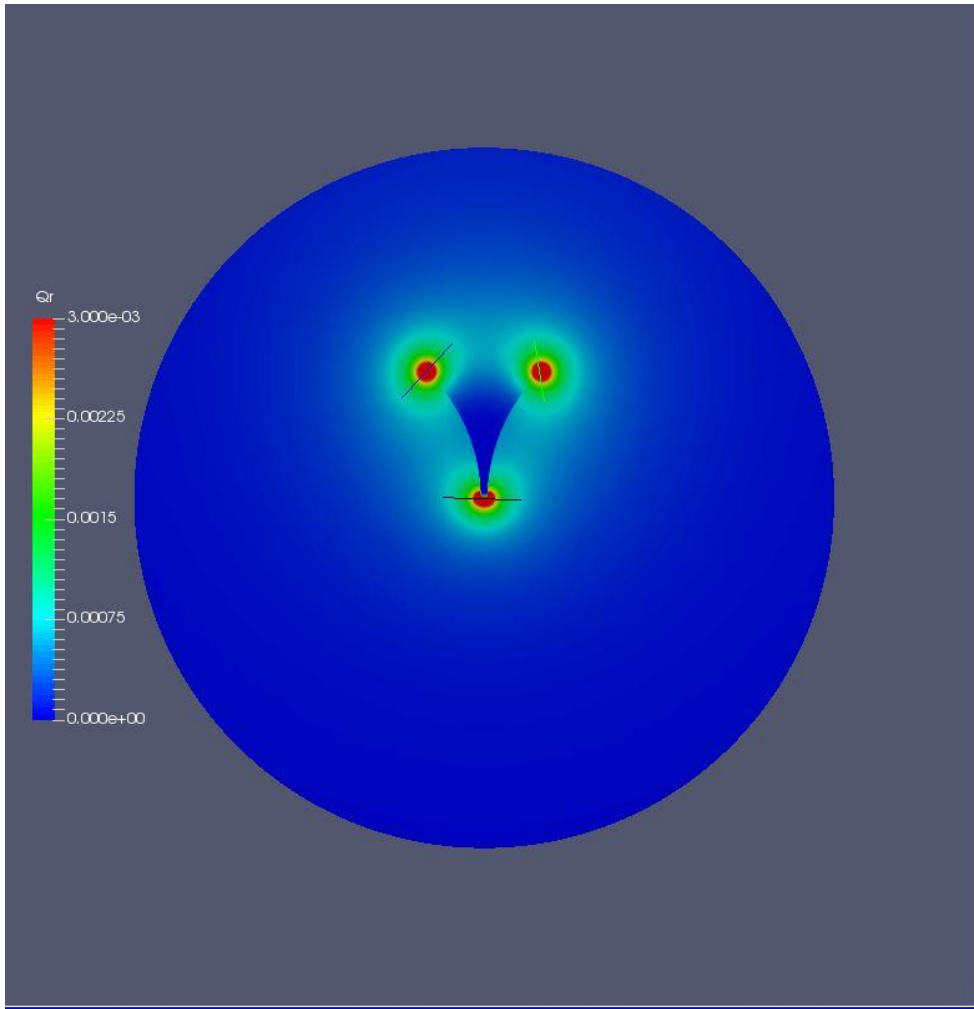


Q_r Visualization on circle

Using Elmer software

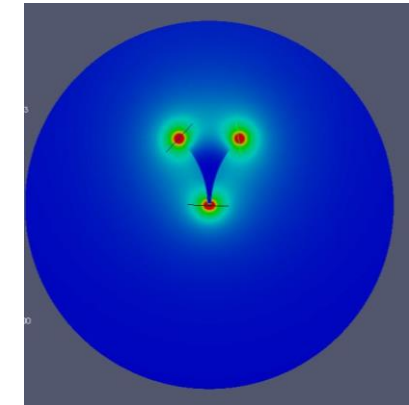
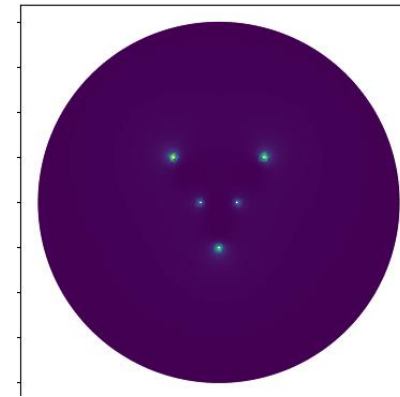


Using Elmer software



$$\sigma \Delta \phi = \delta_0 \text{ on } \Omega$$

$$\delta_0 = \frac{1}{2\sqrt{\pi\epsilon}} e^{-\frac{|x|^2}{\epsilon}}$$



Theorem (Smoothness¹): If $u \in C(\Omega)$ satisfies the mean value property for each ball $B(\mathbf{x}, r) \subset \Omega$, then $u \in C^\infty(\Omega)$

In Proof:

$$u^\epsilon(\mathbf{x}) = \int_{\Omega} \eta_\epsilon(\mathbf{x} - \mathbf{y}) u(\mathbf{y}) d\mathbf{y}$$

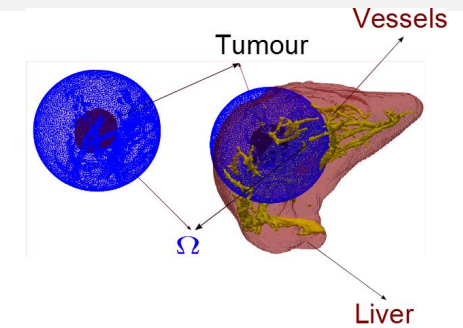
$$\Omega_\epsilon = \{\mathbf{x} \in \Omega: \text{dist}(\mathbf{x}, \partial\Omega) > \epsilon\}$$

$$u^\epsilon = u \text{ in } \Omega_\epsilon$$

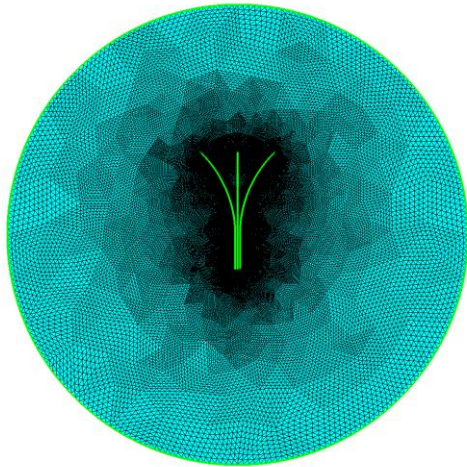
1. Evans, Partial Differential Equations, AMS, 2010, Page 28

Bioheat Equation¹

$$\rho C \frac{\partial T}{\partial t} = k \Delta T + \omega_b \rho_b C_b (T_a - T) + Q_r \text{ on } \Omega$$



Point Source Model

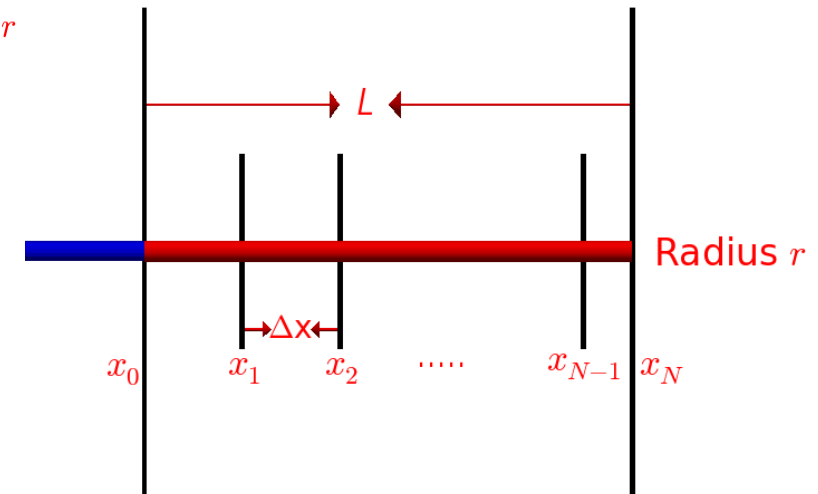
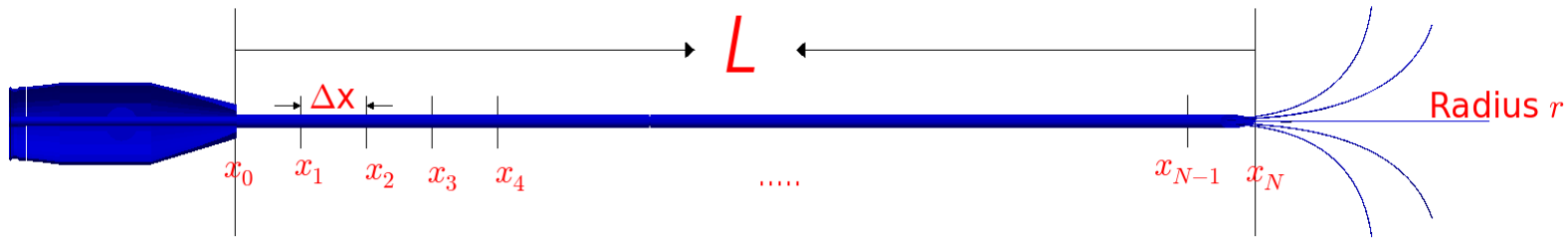


$$P(\vec{x}) = \frac{\sum_{tip} \alpha_{tip} \exp\left(-\frac{\|\vec{x} - \vec{x}_{tip}\|^2}{2\sigma^2}\right)}{\sum_{tip} \alpha_{tip} (\sigma\sqrt{2\pi})^3}$$

$$Q_r = \sum P(\vec{x}) * power$$

1. H. H. Pennes, Analysis of tissue and arterial blood temperature in the resting human forearm, J. Appl. Physio. 85(1):93-102, 1948
2. O'Neill DP, Peng T et al (2011) A three-state mathematical model of hyperthermic cell death. Ann Biomed Eng 39(1):570-579

Joule Heat Model



$$\phi_e(\vec{x}) = \int_0^L \frac{q_e(x') dx'}{4\pi\epsilon |\vec{x} - x'|} = \frac{2\pi r}{4\pi\epsilon} \sum_{j=1}^N q_j \int_{I_j} \frac{dx'}{|\vec{x} - x'|}$$

$$q_j = \begin{cases} q_a, & j = 2, 3, \dots, N - 1 \\ q_b, & j = 1, N \end{cases}$$

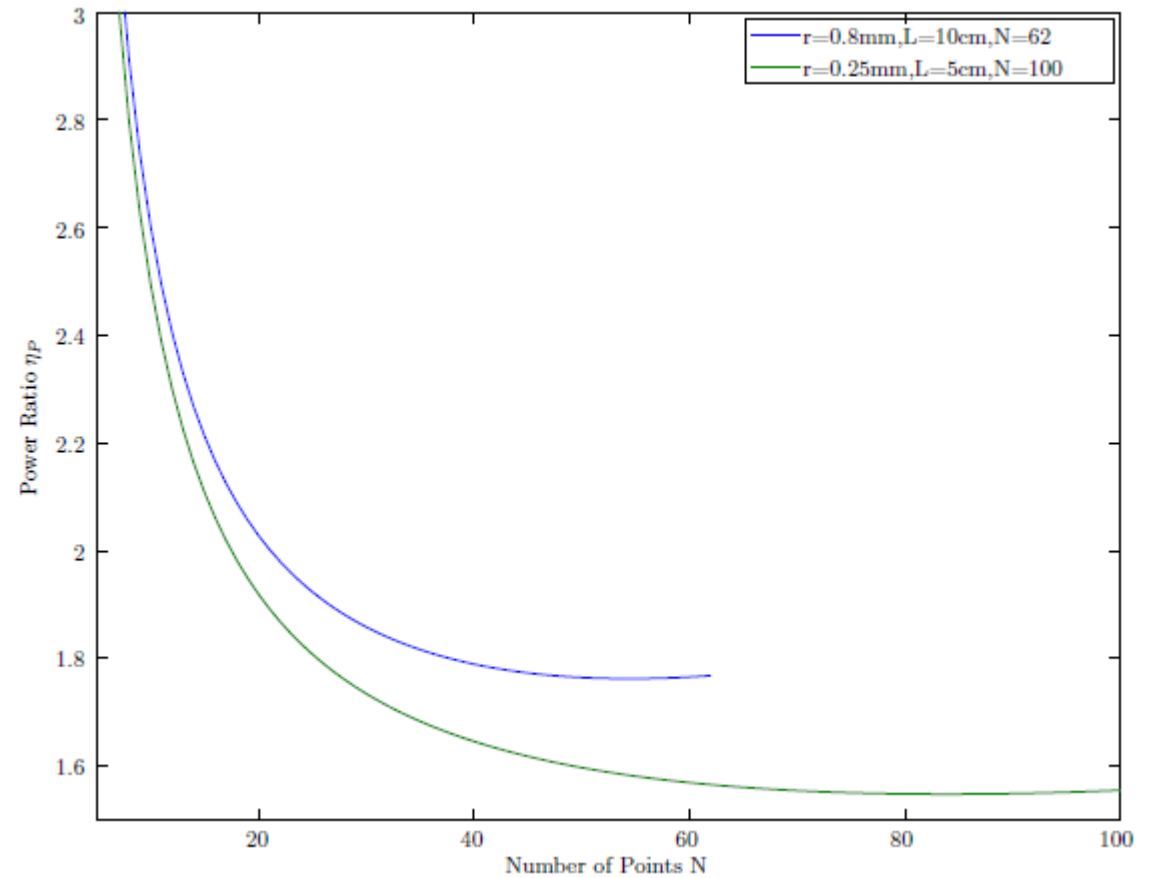
Alternatively when number of points known(k): $k \leq N$

$$\eta_P = \frac{\text{Power deposition at ends}}{\text{Power deposition at middle}} = \frac{P_{\text{end}}}{P_{\text{mid}}}$$

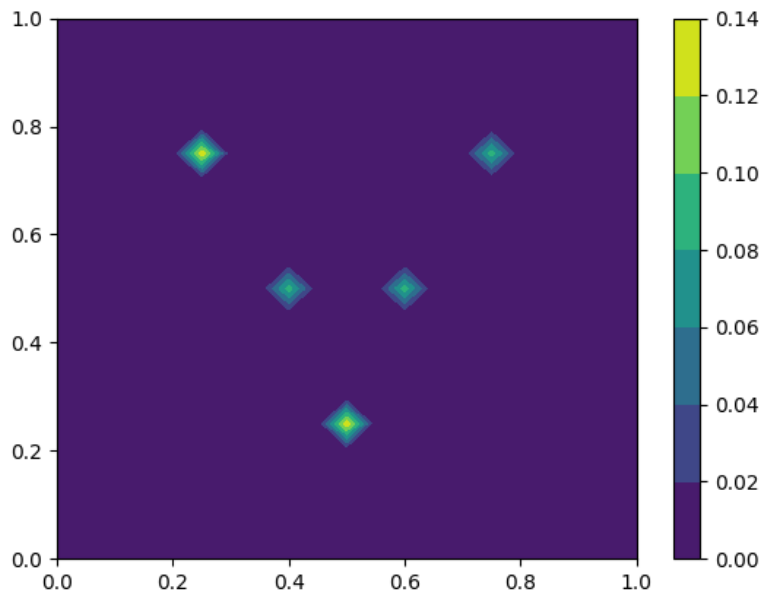
$$\eta_P = \frac{P_{\text{end}}}{P_{\text{mid}}} = \frac{P_b + \left(\frac{N}{k} - 1\right) P_a}{\frac{N}{k} P_a}$$

$$\eta_P = \begin{cases} 1.76 & L = 10\text{cm}, r = 0.8\text{mm} \\ 1.5 & r = 0.25\text{mm}, L = 5\text{cm} \end{cases}$$

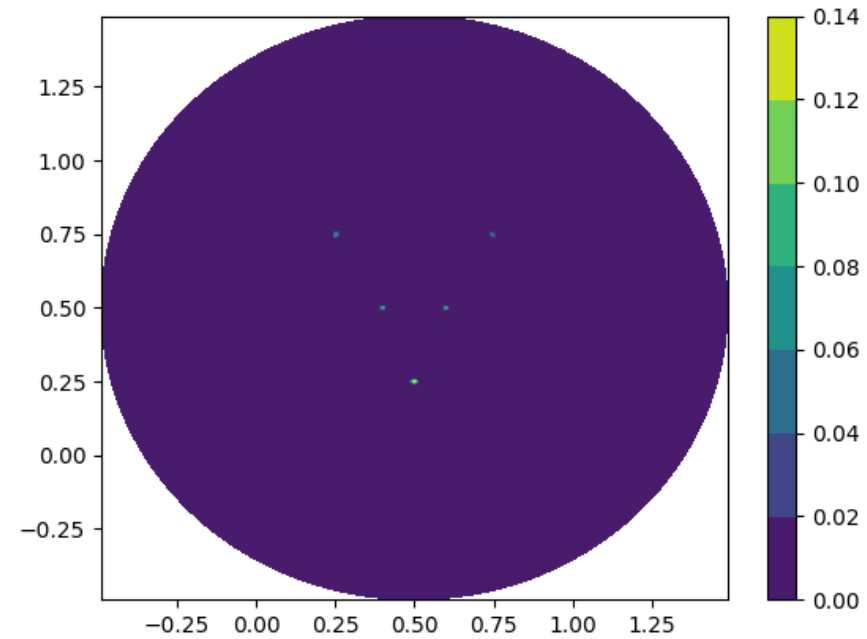
$$\alpha_{\text{tip}} = \begin{cases} 1.5 & \text{end tips} \\ 1.0 & \text{middle tips} \end{cases}$$



Using FeniCS software



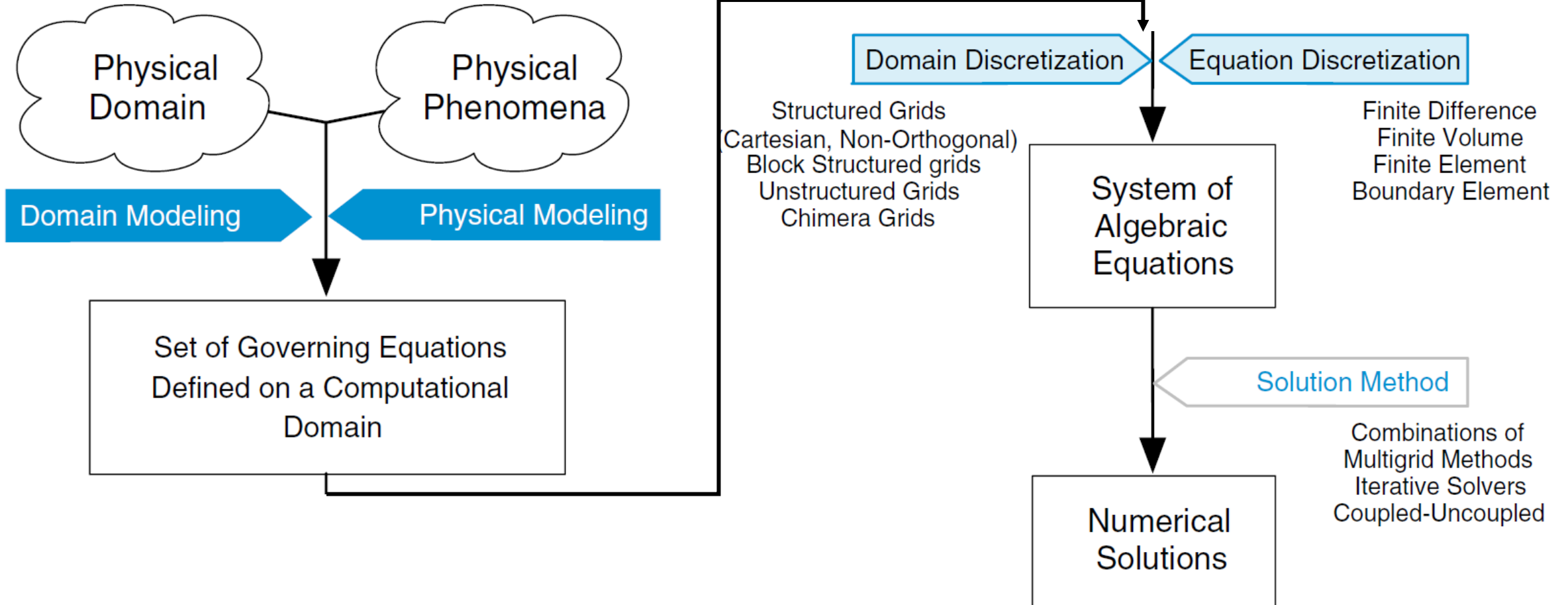
Q_r Visualization on unit square



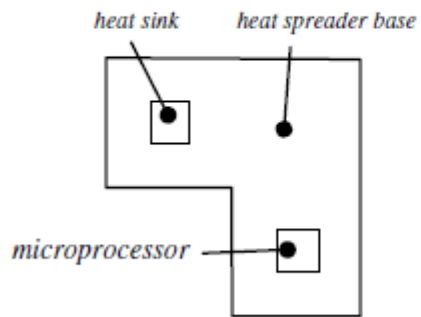
Q_r Visualization on circle

Numerical PDEs: General Idea

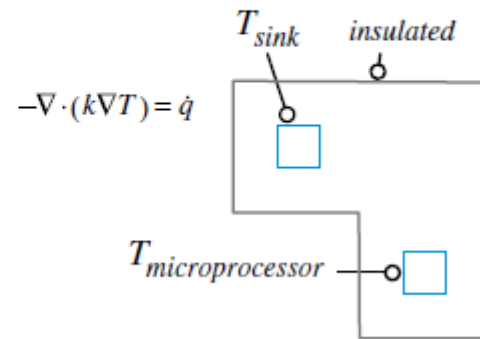
Discretization Process



Domain Modeling



Physical Modeling

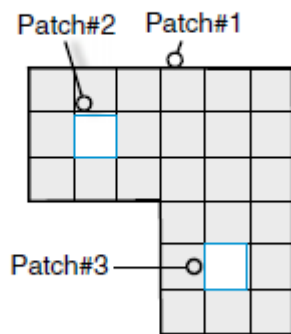


Equations Discretization

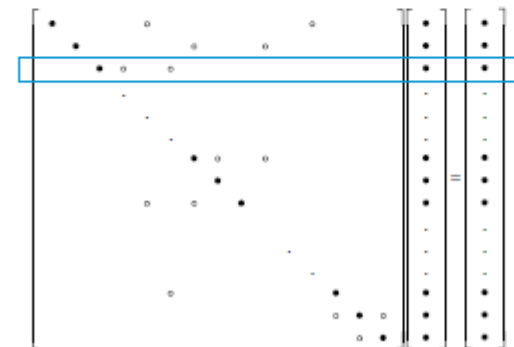
$$\underbrace{\frac{\partial(\rho\phi)}{\partial t}}_{\text{transient term}} + \underbrace{\nabla \cdot (\rho\mathbf{v}\phi)}_{\text{convective term}} = \underbrace{\nabla \cdot (\Gamma\nabla\phi)}_{\text{diffusion term}} + \underbrace{S_c}_{\text{source term}}$$

$$a_C \phi_C + \sum_{F \sim NB(C)} a_F \phi_F = b_C$$

Domain Discretization



Solution Method

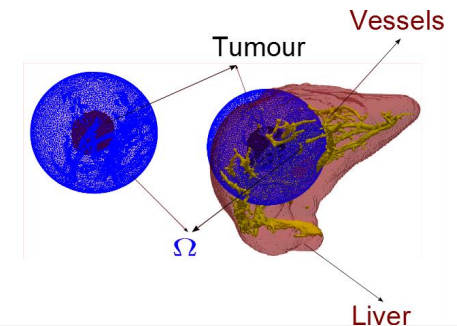


Bioheat Equation¹

$$\rho C \frac{\partial T}{\partial t} = k \Delta T + \omega_b \rho_b C_b (T_a - T) + Q_r \text{ on } \Omega$$

$$h_c T + k \frac{\partial T}{\partial \vec{n}} = h_c T_\infty \text{ on vessels boundary}$$

$$T = T_0 \text{ on } \partial\Omega$$



Cell Death Model²

$$\frac{dA}{dt} = -k_f e^{\frac{T}{T_k}} (1 - A) A + k_b (1 - A - D)$$

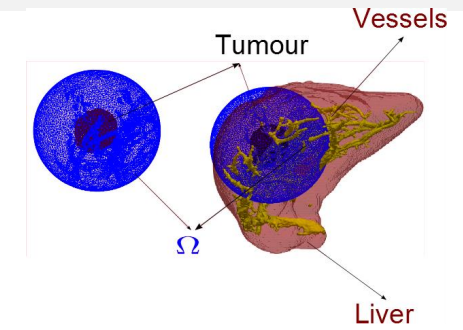
$$\frac{dD}{dt} = k_f e^{\frac{T}{T_k}} (1 - A) (1 - A - D)$$

$$A(0) = 0.99, D(0) = 0.0$$

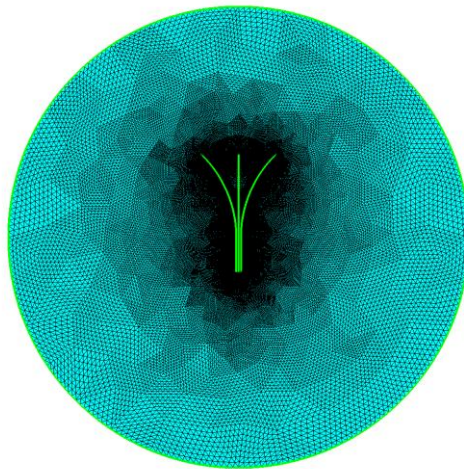
1. H. H. Pennes, Analysis of tissue and arterial blood temperature in the resting human forearm, J. Appl. Physio. 85(1):93-102, 1948
2. O'Neill DP, Peng T et al (2011) A three-state mathematical model of hyperthermic cell death. Ann Biomed Eng 39(1):570-579

Bioheat Equation¹

$$\rho C \frac{\partial T}{\partial t} = k \Delta T + \omega_b \rho_b C_b (T_a - T) + Q_r \text{ on } \Omega$$



Joule Heat Model



$$\sigma \Delta \phi = 0 \text{ on } \Omega$$

$$\phi = \begin{cases} \phi_r \text{ on NeedleTips} \\ \phi_c \text{ on Circularboundary} \end{cases}$$

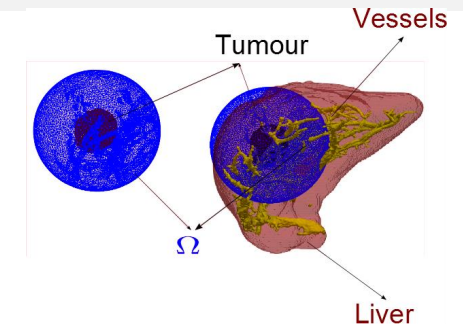
$$\frac{\partial \phi}{\partial n} = 0 \text{ on Needle shaft}$$

$$Q_r = \sigma (|\nabla \phi|^2)$$

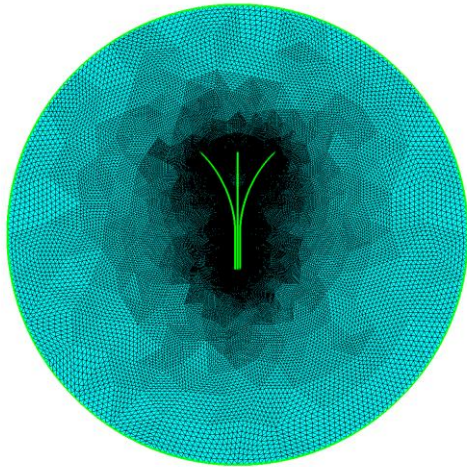
1. H. H. Pennes, Analysis of tissue and arterial blood temperature in the resting human forearm, J. Appl. Physio. 85(1):93-102, 1948
2. O'Neill DP, Peng T et al (2011) A three-state mathematical model of hyperthermic cell death. Ann Biomed Eng 39(1):570-579

Bioheat Equation¹

$$\rho C \frac{\partial T}{\partial t} = k \Delta T + \omega_b \rho_b C_b (T_a - T) + Q_r \text{ on } \Omega$$



Point Source Model



$$P(\vec{x}) = \frac{\sum_{tip} \alpha_{tip} \exp\left(-\frac{\|\vec{x} - \vec{x}_{tip}\|^2}{2\sigma^2}\right)}{\sum_{tip} \alpha_{tip} (\sigma\sqrt{2\pi})^3}$$

$$Q_r = \sum P(\vec{x}) * power$$

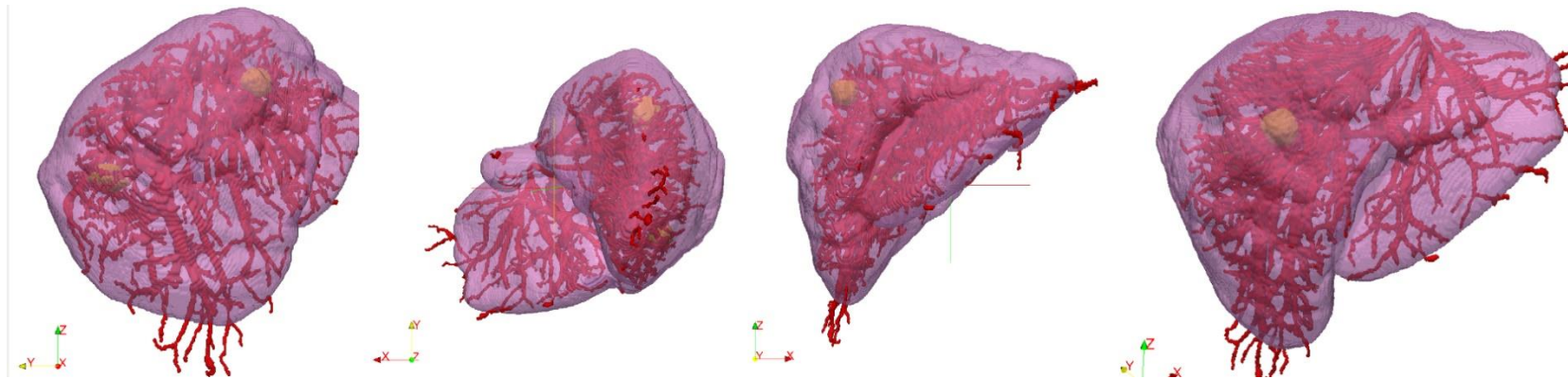
1. H. H. Pennes, Analysis of tissue and arterial blood temperature in the resting human forearm, J. Appl. Physio. 85(1):93-102, 1948
2. O'Neill DP, Peng T et al (2011) A three-state mathematical model of hyperthermic cell death. Ann Biomed Eng 39(1):570-579

Validation Phase

Simulation Accuracy

RFA Validation Study:

- RFA simulation has been tested using over 100 meshes
- Patient data used for each was the same



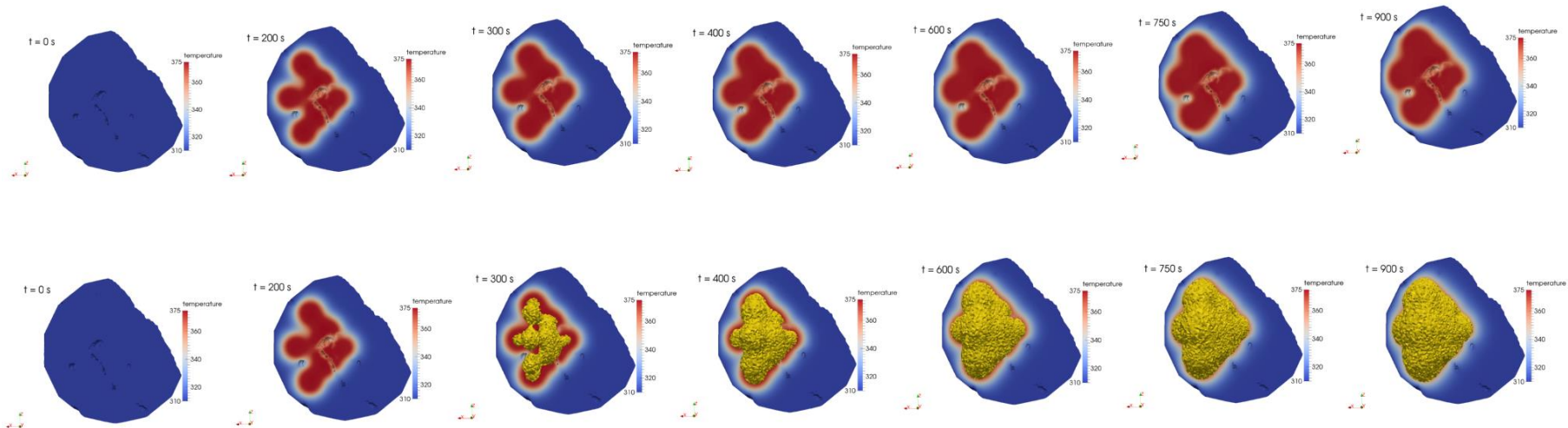
- Report filled out by physicians who conducted the procedure used to replicate protocol as accurately as possible

Simulation parameters:

- As well as same patient data used for each simulation, identical input values were used for following parameters:
 - Input power = 150 Watts
 - Spherical domain centred on tumour location with 30mm radius
 - Simulation ran for 225 4 second timesteps
- Meshing parameters varied as follows:
 - Nearfield = 0.1 – 2.0
 - Farfield = 0.4 – 5.0
 - Zonefield = 0.5 – 5.0

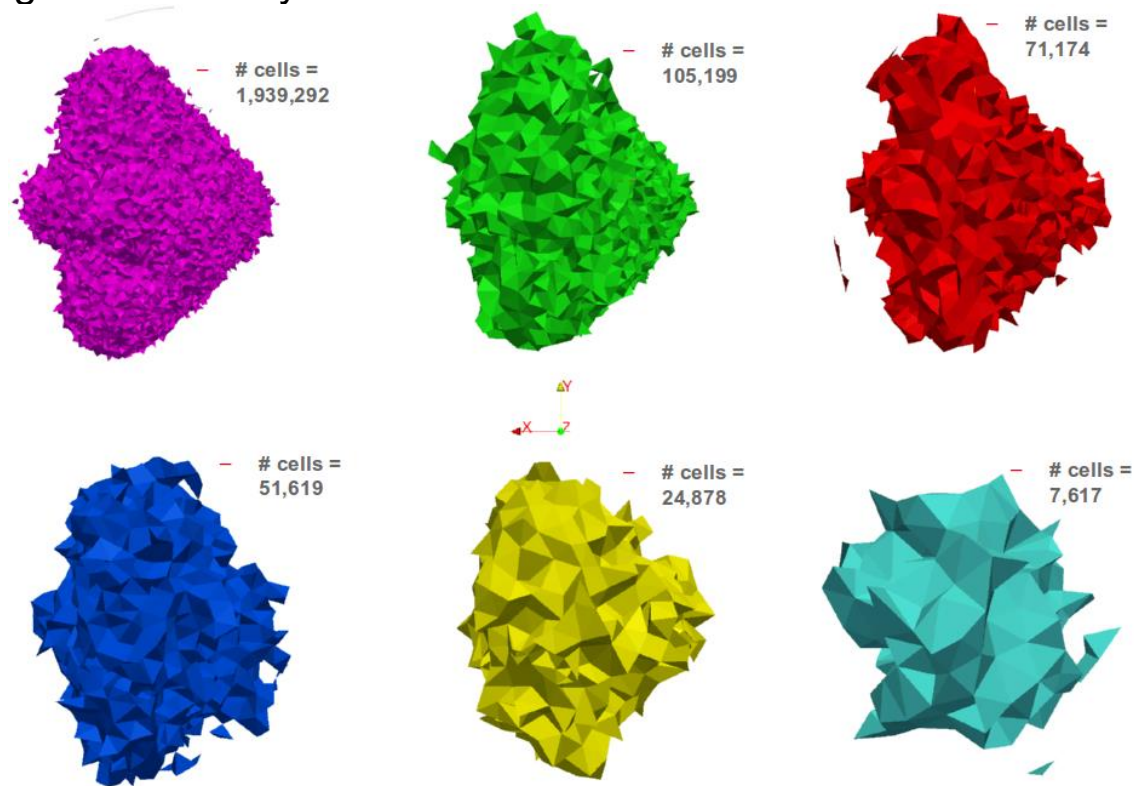
Lesion growth:

- The growth of the lesion during the procedure is shown below:



Results:

- Predicted lesion of each simulation compared to lesion of finest mesh – influence of increasing mesh density clear:



Volume Deviation

$$DSC = \frac{2 |V_{se} \cap V_{si}|}{|V_{se}| + |V_{si}|}$$

$$RVD = \left| \frac{|V_{se}|}{|V_{si}|} - 1 \right|$$

$$SN = \frac{|V_{se} \cap V_{si}|}{|V_{se}|}$$

$$VOE = \frac{|V_{si} \cap V_{se}|}{|V_{si} \cup V_{se}|}$$

$$PPV = \frac{|V_{se} \cap V_{si}|}{|V_{si}|}$$

V_{se} : Segmented lesion volume
 V_{si} : Simulated lesion volume

Surface Deviation

$\vec{p}_i = (p_{ix}, p_{iy}, p_{iz})$: point at the surface of the simulated lesion

R : Segmented lesion surface

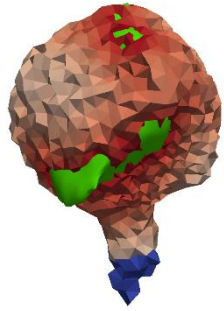
$$d_i = d(\vec{p}_i, R) = \min_j \left\{ \sqrt{(p_{ix} - r_{jx})^2 + (p_{iy} - r_{jy})^2 + (p_{iz} - r_{jz})^2} \right\}$$

$$AAE = \frac{\sum w_i |d_i|}{\sum w_i}$$

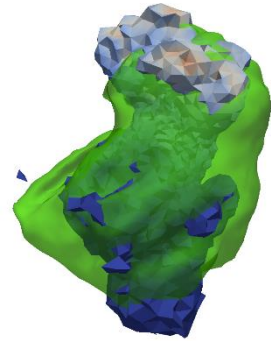
Simulated Lesion matches with Segmented lesion only if

AAE < 3.5mm

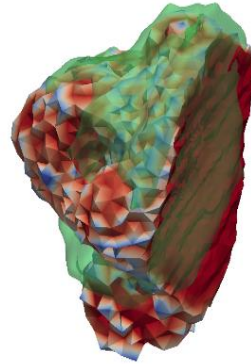
RVD < 30%, DSC, SN, PPV > 70% or VOE > 70%



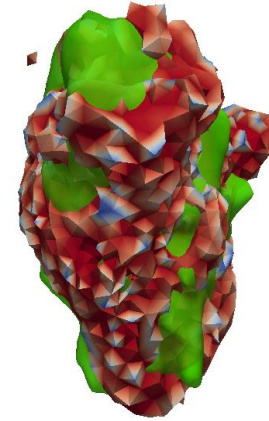
RVD: 18
Surf Dev: 2.28



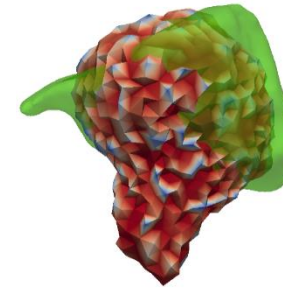
RVD: 74
Surf Dev: 3.09



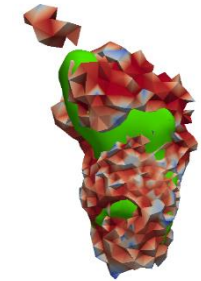
RVD: 6.67
Surf Dev: 2.88



RVD: 0.003
Surf Dev: 4.57



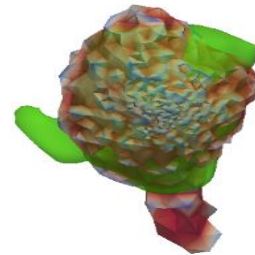
RVD: 0.61
Surf Dev: 2.74



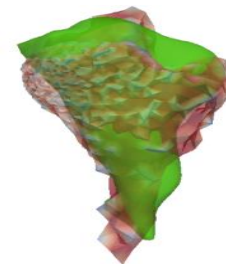
RVD: 55.71
Surf Dev: 1.88



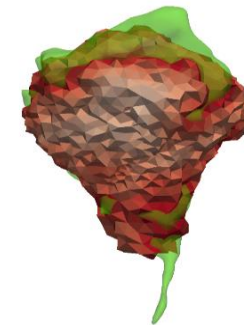
RVD: 0.58
Surf Dev: 2.37



RVD: 3.56
Surf Dev: 1.53



RVD: 7.94
Surf Dev: 1.79



RVD: 21.64
Surf Dev: 2.57

Microwave Ablation

Generic Open-end Simulation, Environment for Minimally Invasive Cancer Treatment

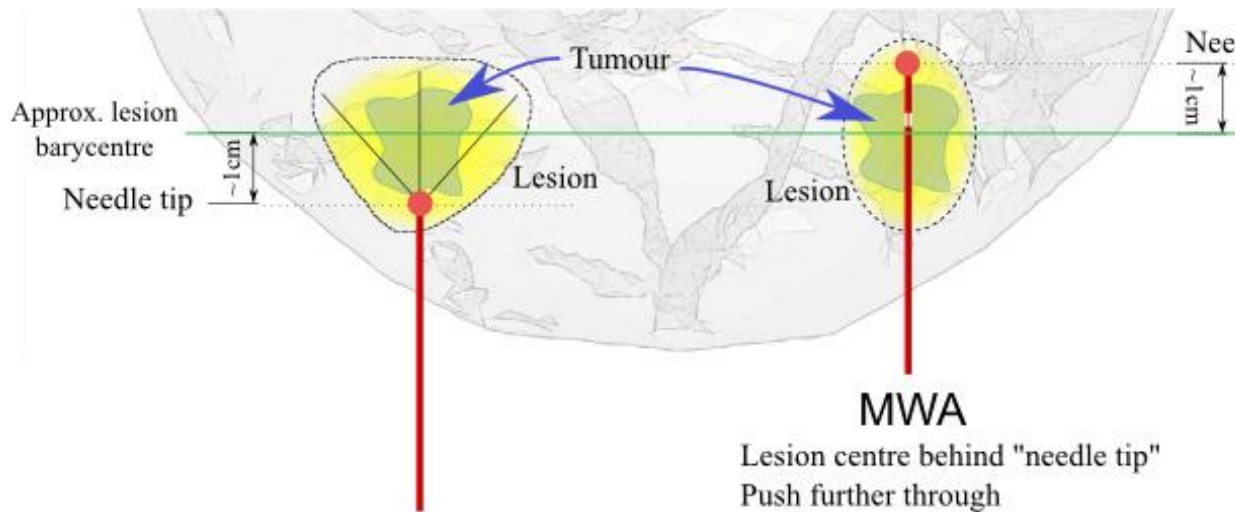
<http://www.gomsart-project.eu>

<http://smart-mict.eu>



Rs.~28 Crores

Generic Open-end Simulation, Environment for Minimally Invasive Cancer Treatment



RFA

Lesion centre ahead of "needle tip"
Don't push as far through

MWA

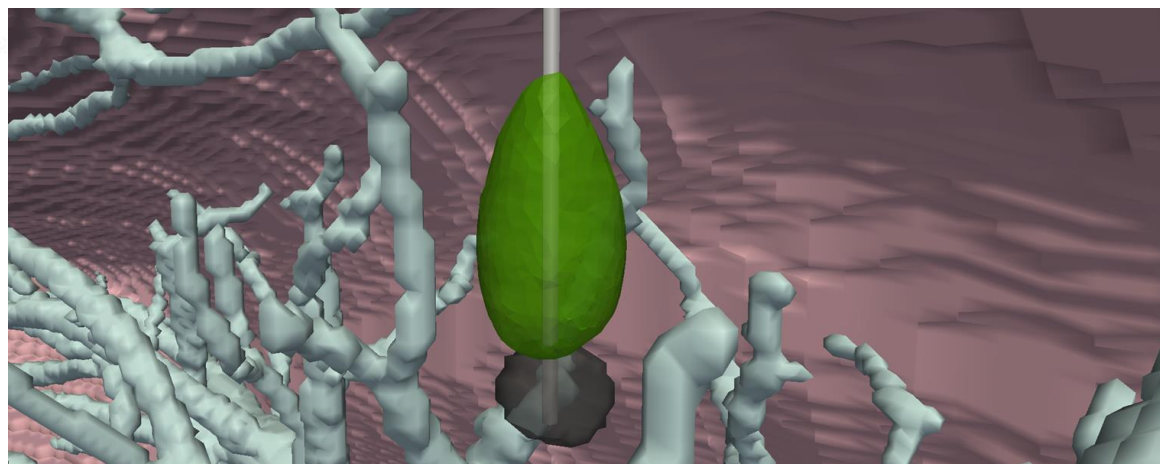
Lesion centre behind "needle tip"
Push further through

$$\nabla \times \left[\left(\epsilon_r - i \frac{\sigma}{\omega \epsilon_0} \right)^{-1} \nabla \times \mathbf{H} \right] - \mu_r k_0^2 \mathbf{H} = 0$$

Importance of aligning offsetting needle tip according to tumour location.

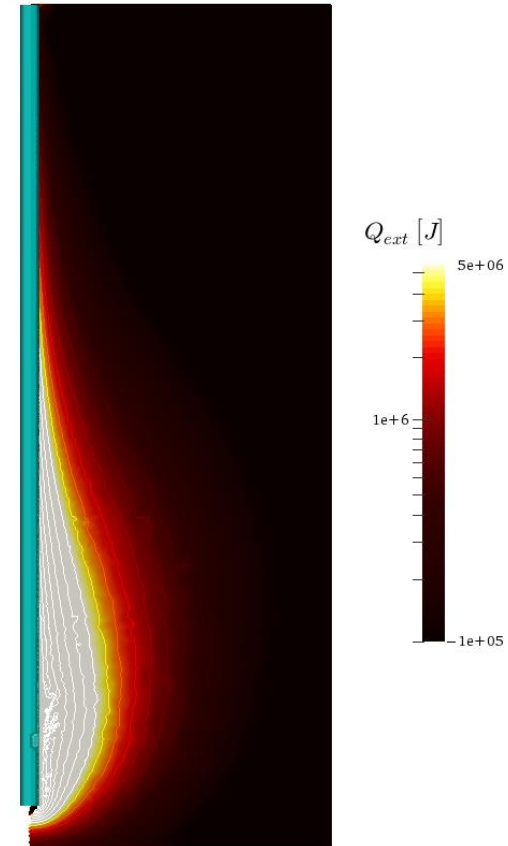
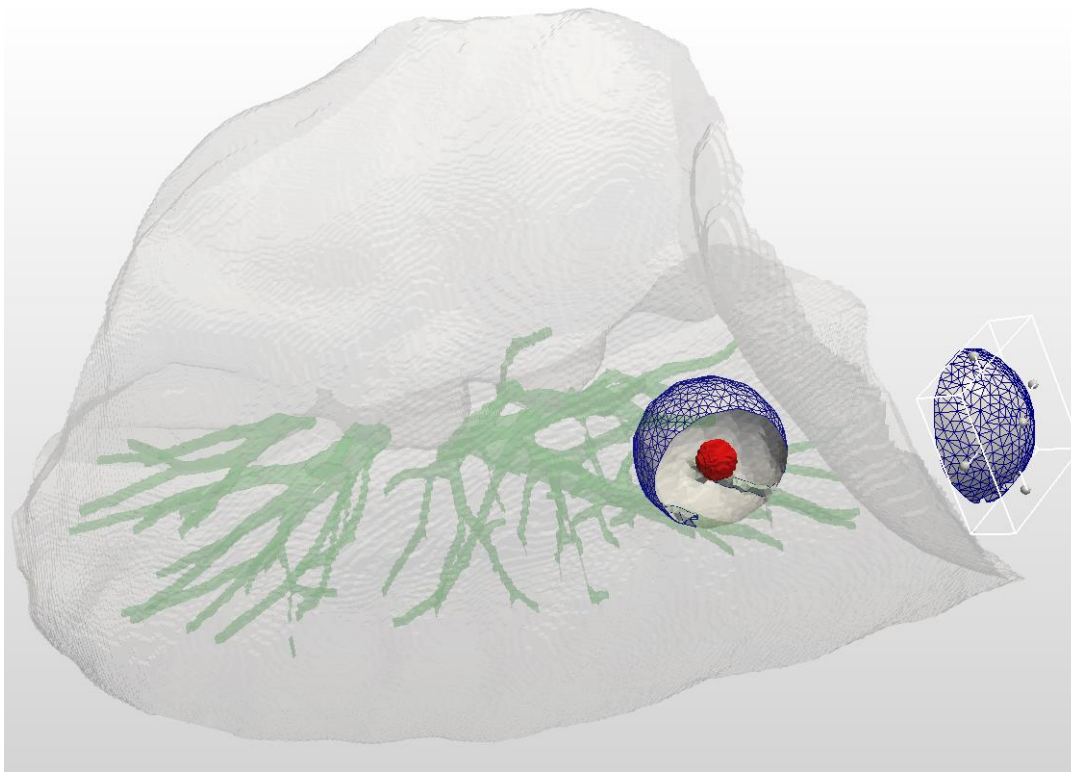
The MWA lesion shown below is generated at low power (~10W) and demonstrates effect of separate tumour tissue values at these ratings

However, at higher power levels, the coupling of temperature and tissue electric properties in the **MWA** simulation are important to represent the physical processes in Go-Smart clinical settings



Tumour (black); Vessels (blue); Lesion (green) Lung wall (pink); Needle (grey)

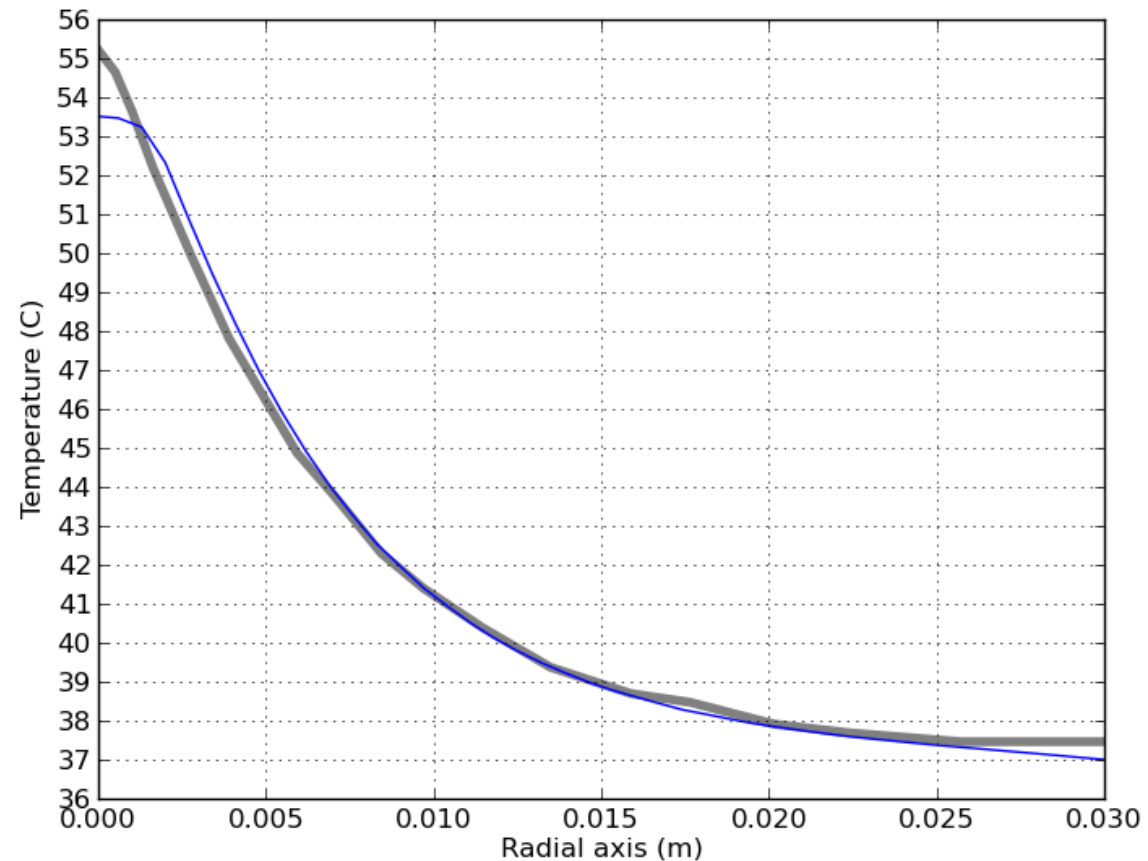
Generic Open-end Simulation, Environment for Minimally Invasive Cancer Treatment



Generic Open-end Simulation, Environment for Minimally Invasive Cancer Treatment

Microwave Ablation

- *Validation within Go-Smart Simulation Framework*
 - ❑ *Gas, 2012*
 - ❑ *COMSOL-based*
 - ❑ *3W steady-state*
 - ❑ *No vessels*



Gas, 2012 – Grey; Go-Smart Simulation - Blue

Generic Open-end Simulation, Environment for Minimally Invasive Cancer Treatment

CGAL Meshing

- ✎ Generates a large number of random points within the computational domain
- ✎ Determines a characteristic element length (L_c) at each of these points
- ✎ If point is sufficiently close to a previous point, it will be assigned the same L_c value
- ✎ L_c between input values: FarField (FF), ZoneField (ZF) and NearField (NF)
- ✎ Exact L_c determined based on a points' distances to important bodies
- Implicit_domain_function computes point's distance from
 - Domain extent
 - Vasculature
 - User-defined centre
 - Tumour edge (zone field)
- ⊗ Labeled_domain_function adapted to incorporate Implicit_domain_function and to align tetrahedra along subvolume boundaries (such as tumours)
- ⊗ Minimum of these distances used to interpolate between NF or ZF and FF for L_c

Generic Open-end Simulation, Environment for Minimally Invasive Cancer Treatment

CGAL Meshing

- ❖ The mesher has been tested extensively – 15 meshes generated from various geometry:
- ❖ Capable of consistently generating usable meshes for any geometrical input
- ❖ User can control mesh location, density and shape using xml input file

Typical number of elements in mesh ~ 250,000 but can vary widely depending on input parameters

User can choose if needle is removed from mesh

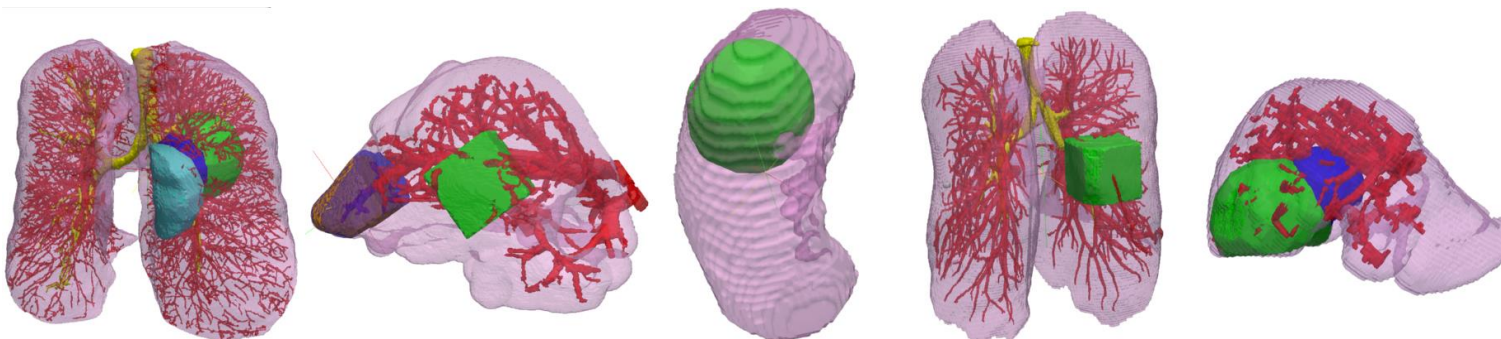
Mesh density controlled by varying Nearfield, Farfield and Zonefield parameters

Tumours can be set as zones distinct from the rest of the mesh

Occasionally there are errors in the mesh

Zero volume or even negative volume elements

Numerical issues in calculating the minimum dihedral angle

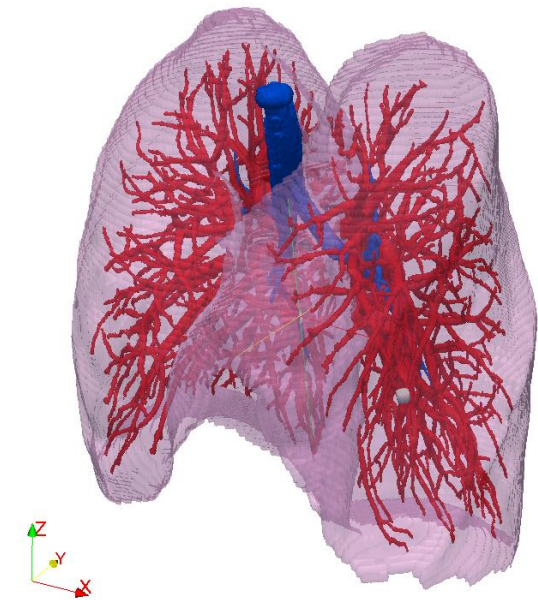


Generic Open-end Simulation, Environment for Minimally Invasive Cancer Treatment

MWA

- ✓ Spherical domain centred at tumour of 40mm radius used
- ✓ Input power = 10 Watts
- ✓ Nearfield = 0.4 Farfield = 3.0
- ✓ Simulation conducted for 1000 timesteps, 2 seconds each
- ✓ Tissue electrical properties exhibit strong non-linearity with elevated temperatures - work under way to account for this
- ✓ Water content very influential which becomes an issue at temperatures close to 100°C

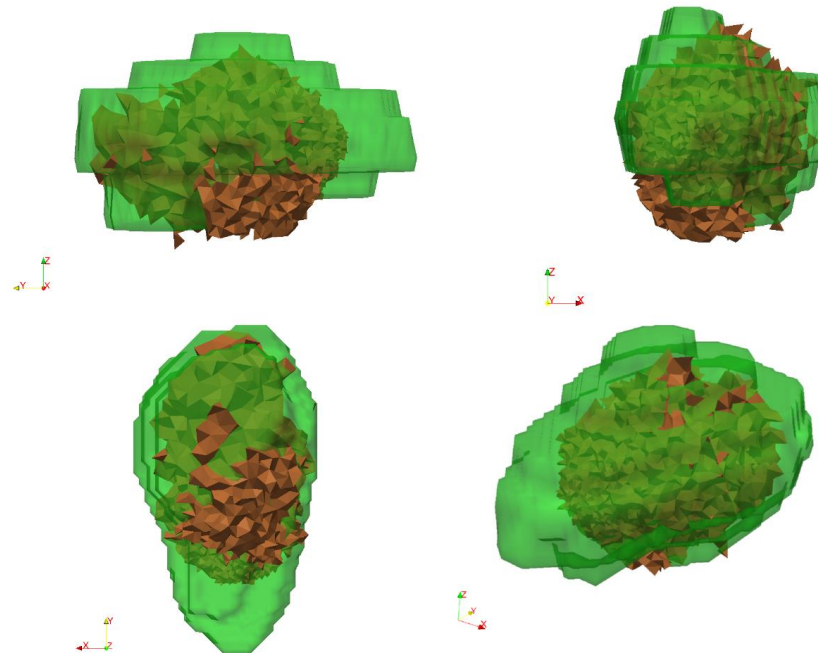
- ❑ Patient data used along with segmented lesion geometrical data
- ❑ Computational domain centred around tumour location
- ❑ Volumes of predicted lesion and segmented one similar



Generic Open-end Simulation, Environment for Minimally Invasive Cancer Treatment

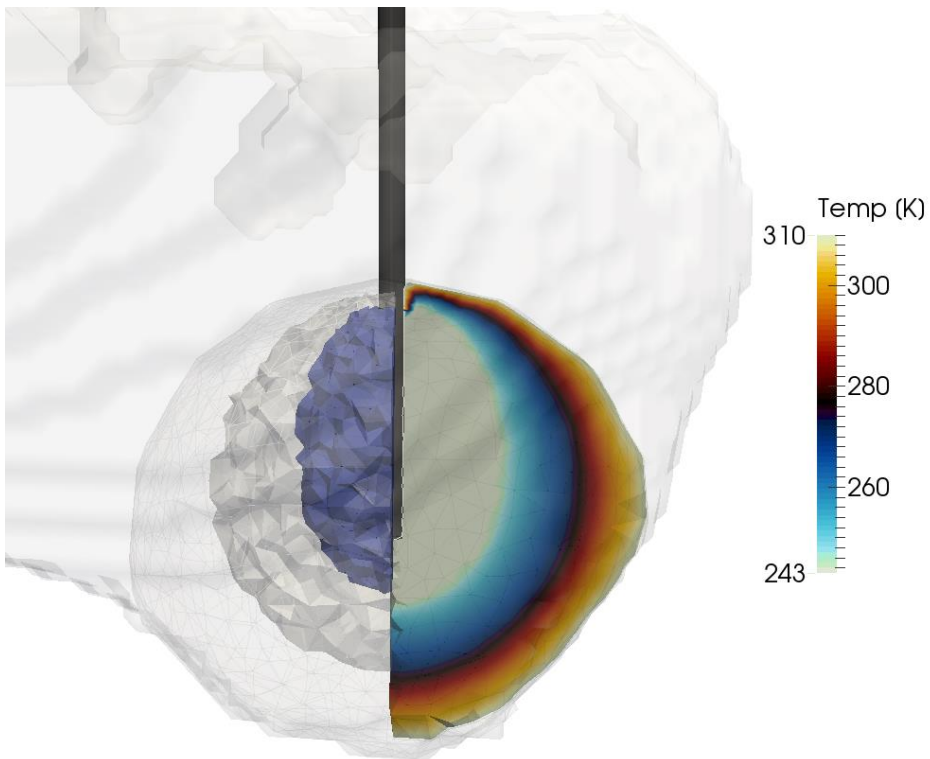
MWA

- ❑ Power tailored for desired temperature, temperature issues since solved
- ❑ Positioning of needle for comparable lesion requires experience with simulation
- ❑ Cells with Dead ≥ 0.8 taken to be in lesion
- ❑ Predicted lesion (orange) of comparable volume to segmented one (green):



Cryoablation

Generic Open-end Simulation, Environment for Minimally Invasive Cancer Treatment



Cryoablation

- *Fluid flowing through a cryogenic needle*
 - Presently, fixed needle surface temperature*
 - Lesion given by -50C isotherm*
 - Computes and accounts for*
 - change of physical properties with phase*

- *White surface – ice ball*
- *Purple surface – lesion extent*

Generic Open-end Simulation, Environment for Minimally Invasive Cancer Treatment

Cryoablation

- *Front-tracking*
- *More stable, efficient*
- *Physical properties change in ice-ball and surrounding mushy zone*
 - ✓ e.g. heat capacity, conductivity, enthalpy, perfusion
- *Temporal phase change model*
- *Incorporates latent heat of phase change by defining an effective heat capacity that varies appropriately around solidus and liquidus temperatures*

$$k_{eff}(T) = \begin{cases} k_s & T < T_s \\ k_s + \frac{1}{2(T_l - T_s)}(k_l - k_s)(T - T_s) & T_s \leq T \leq T_l \\ k_l & T > T_l \end{cases}$$

$$c_{eff}(T) = \begin{cases} c_f, & T < T_s, \\ \frac{c_f + c_u}{2} + \frac{h_{sf}}{2(T_l - T_s)}, & T_s \leq T \leq T_l, \\ c_u, & T > T_l, \end{cases}$$

Generic Open-end Simulation, Environment for Minimally Invasive Cancer Treatment

Cryoablation

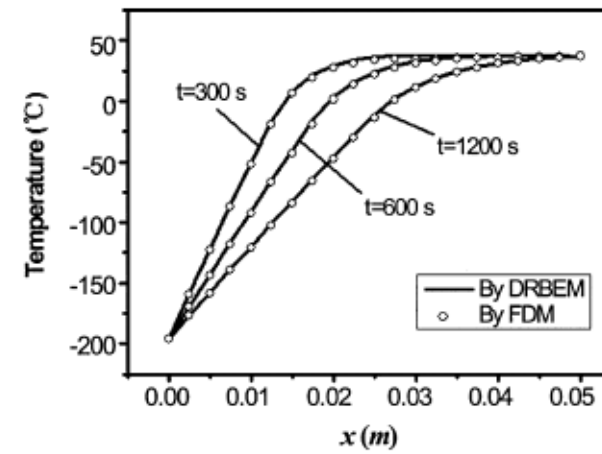
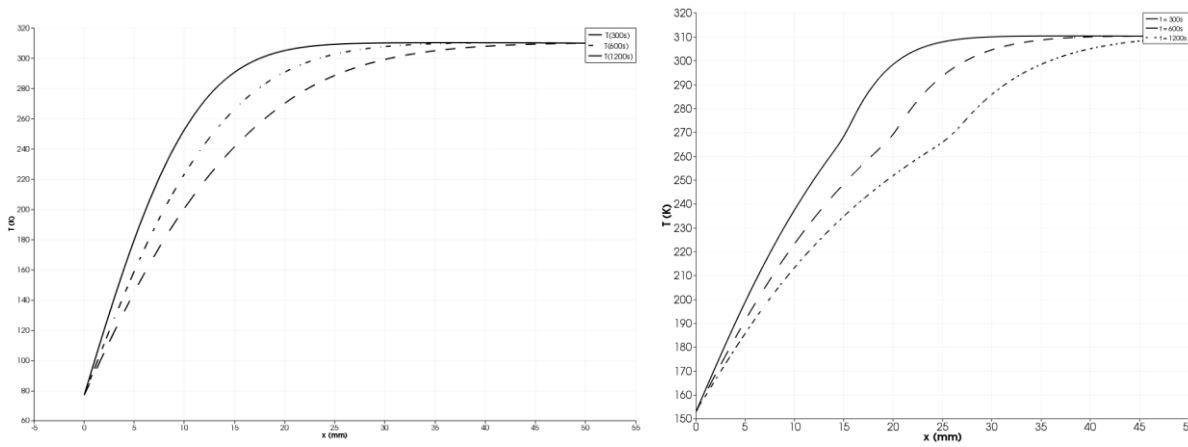
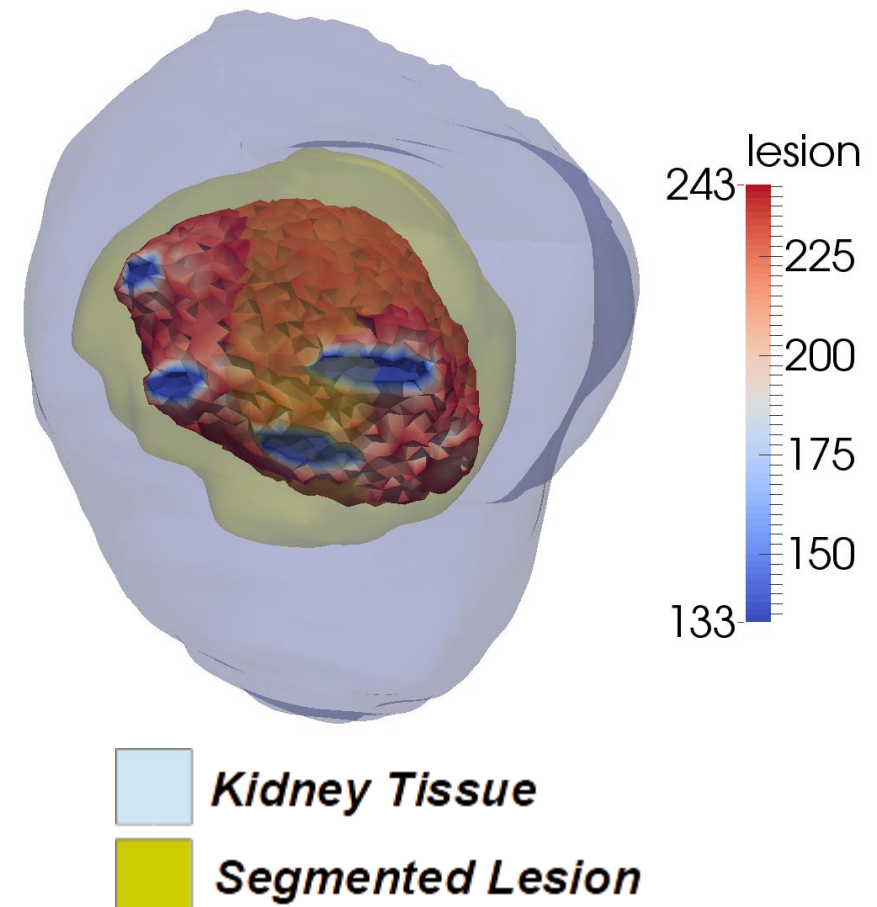


Fig. 4. Temperature distribution at different times for Problem 1.

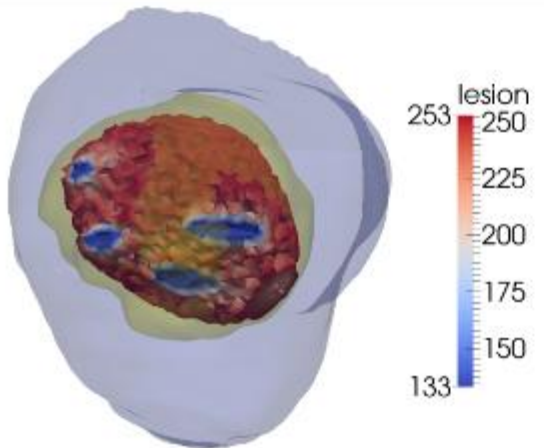
Generic Open-end Simulation, Environment for Minimally Invasive Cancer Treatment

Cryoablation

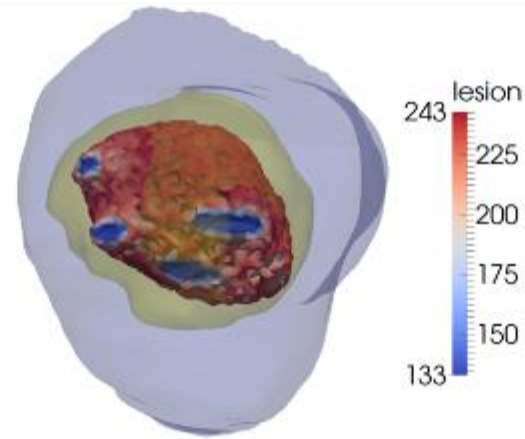
- Freeze-Thaw Cycle
 - 10 min. freezing
 - 1 min. passive thawing
 - 2 min. active thawing
 - (repeat)
- Cells considered dead where tissue temperature below -40°C
- GSSF restart functionality undergoing testing



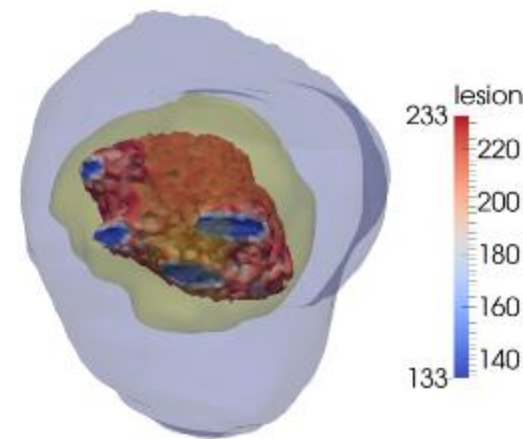
Generic Open-end Simulation, Environment for Minimally Invasive Cancer Treatment



-20°C isotherm



-30°C isotherm



-40°C isotherm

Simulated Time: 26 minutes

Elements: 232,954



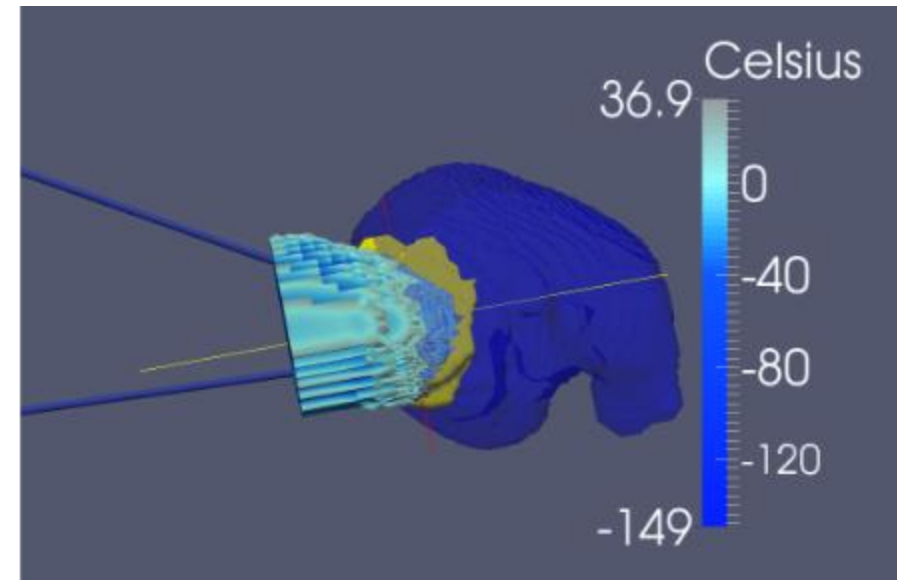
Kidney Tissue



Segmented Lesion

Generic Open-end Simulation, Environment for Minimally Invasive Cancer Treatment

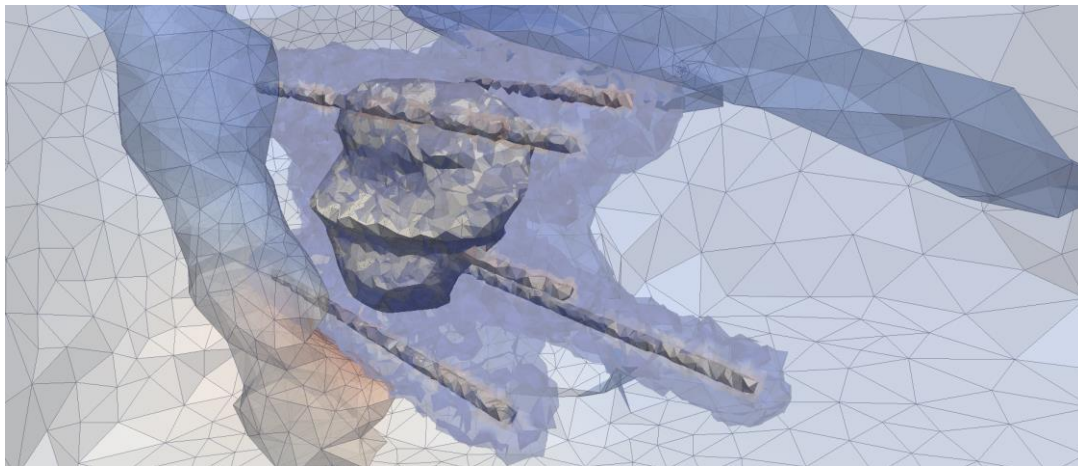
Needles	2
Simulation	26 min
Elements	2,079,334
Runtime	6 min
Processors	8



Irreversible Electroporation

Generic Open-end Simulation, Environment for Minimally Invasive Cancer Treatment

IRE



- *Modeled using simple electric potential solver*
 - Current test - 6 needles
 - Anodes and cathodes; 9 consecutive pairs
 - Calculate cumulative coverage

$$\nabla \cdot (\sigma \nabla \phi) = 0$$

$$\left. \frac{\partial \phi}{\partial n} \right|_{A_i} = V_i$$

$$\left. \frac{\partial \phi}{\partial n} \right|_{C_i} = 0$$

Generic Open-end Simulation, Environment for Minimally Invasive Cancer Treatment

Electric potential:

$$\nabla \cdot (\sigma \nabla \phi) = 0$$

$$E = \frac{1}{2} (\nabla \phi)^2$$

$$\sigma = \begin{cases} \sigma_u & E > E_u \\ \text{lin.int.} & E_l \leq E \leq E_u \\ \sigma_l & E < E_l \end{cases}$$

Active needle pairs:

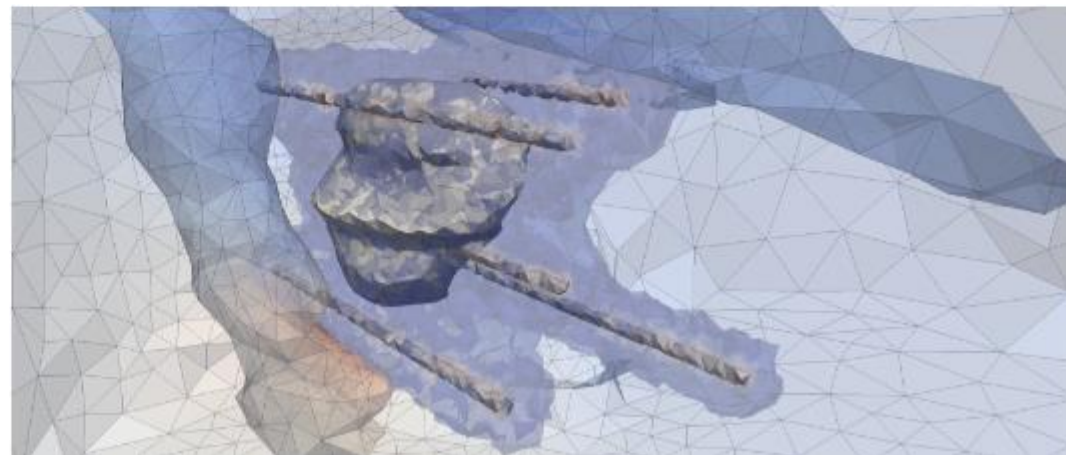
$$\phi = V \quad \text{on anode}$$

$$\phi = 0 \quad \text{on cathode}$$

$$(\nabla \phi) \cdot n = 0 \quad \text{remaining boundaries}$$

Investigating efficient, representative 2D quick simulations for instant feedback.

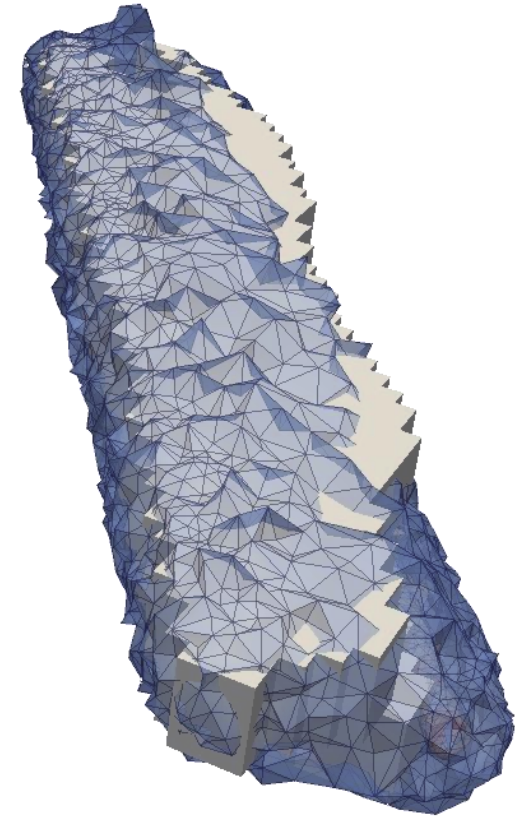
**FE Engines:
Elmer FEM / FEniCS**



Generic Open-end Simulation, Environment for Minimally Invasive Cancer Treatment

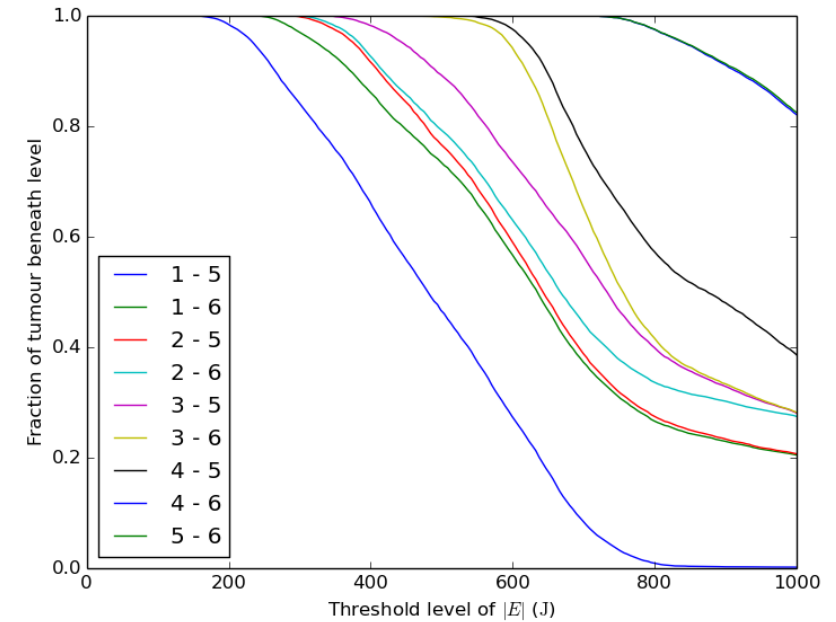
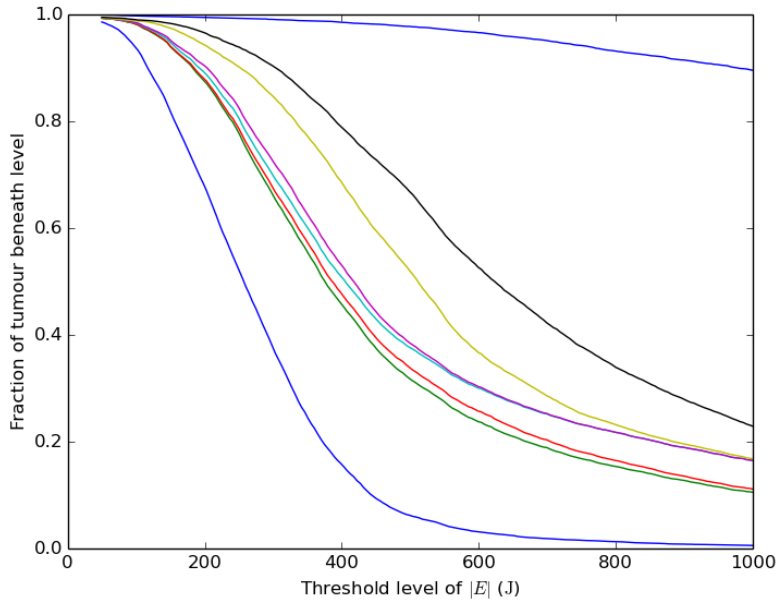
IRE

- *Electrical properties change based on the deposited energy*
- *Final lesion is defined as an isovolume based on a chosen threshold of the local energy maximum over the whole protocol sequence*



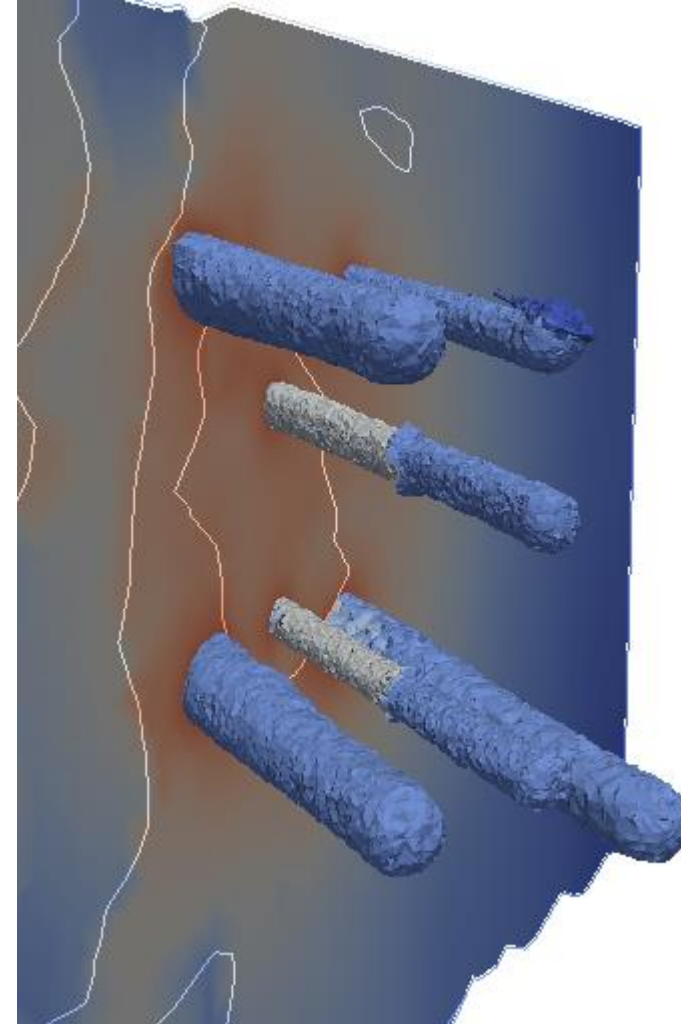
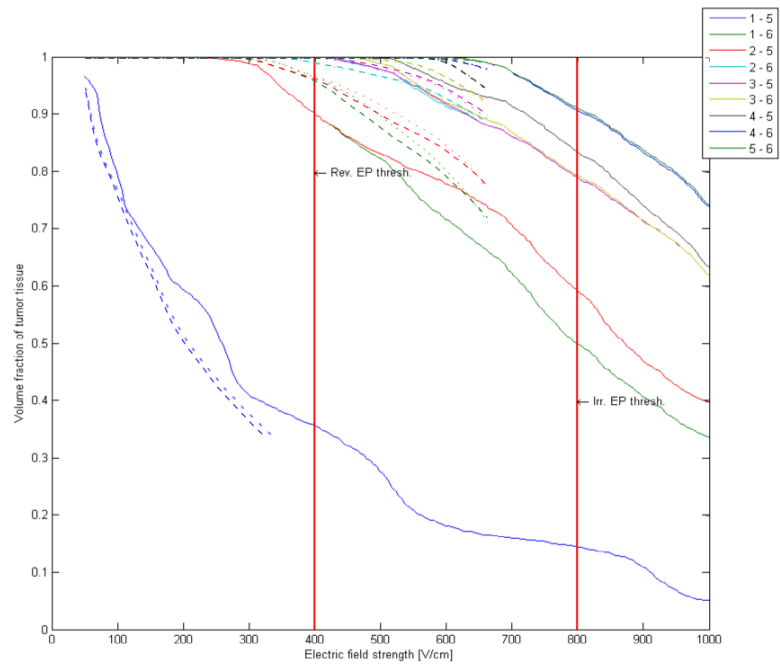
Generic Open-end Simulation, Environment for Minimally Invasive Cancer Treatment

IRE



Generic Open-end Simulation, Environment for Minimally Invasive Cancer Treatment

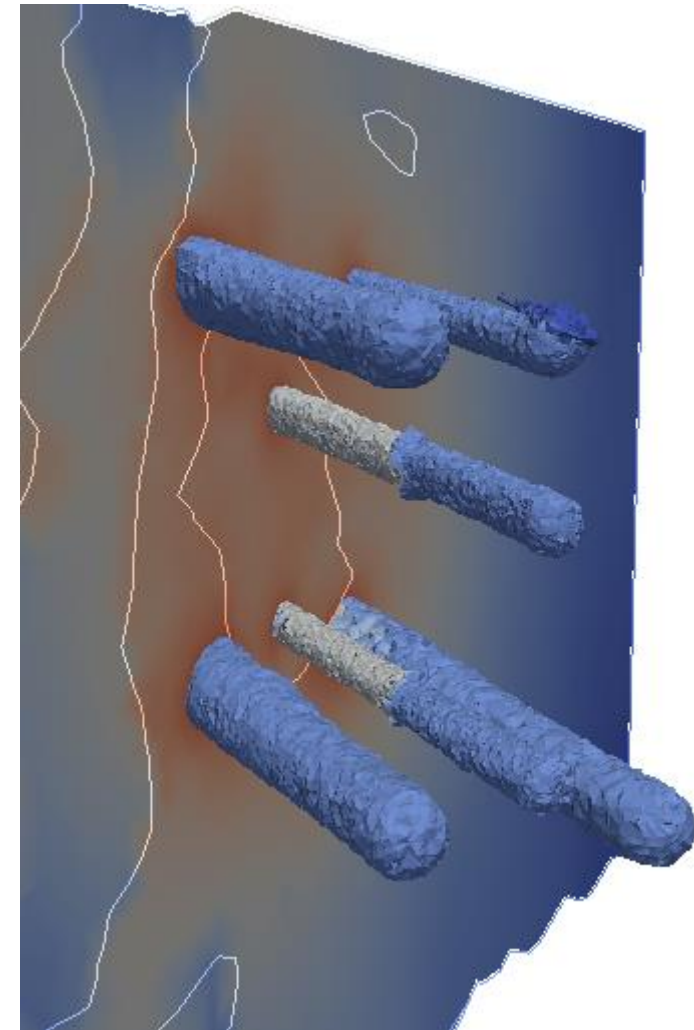
IRE



Generic Open-end Simulation, Environment for Minimally Invasive Cancer Treatment

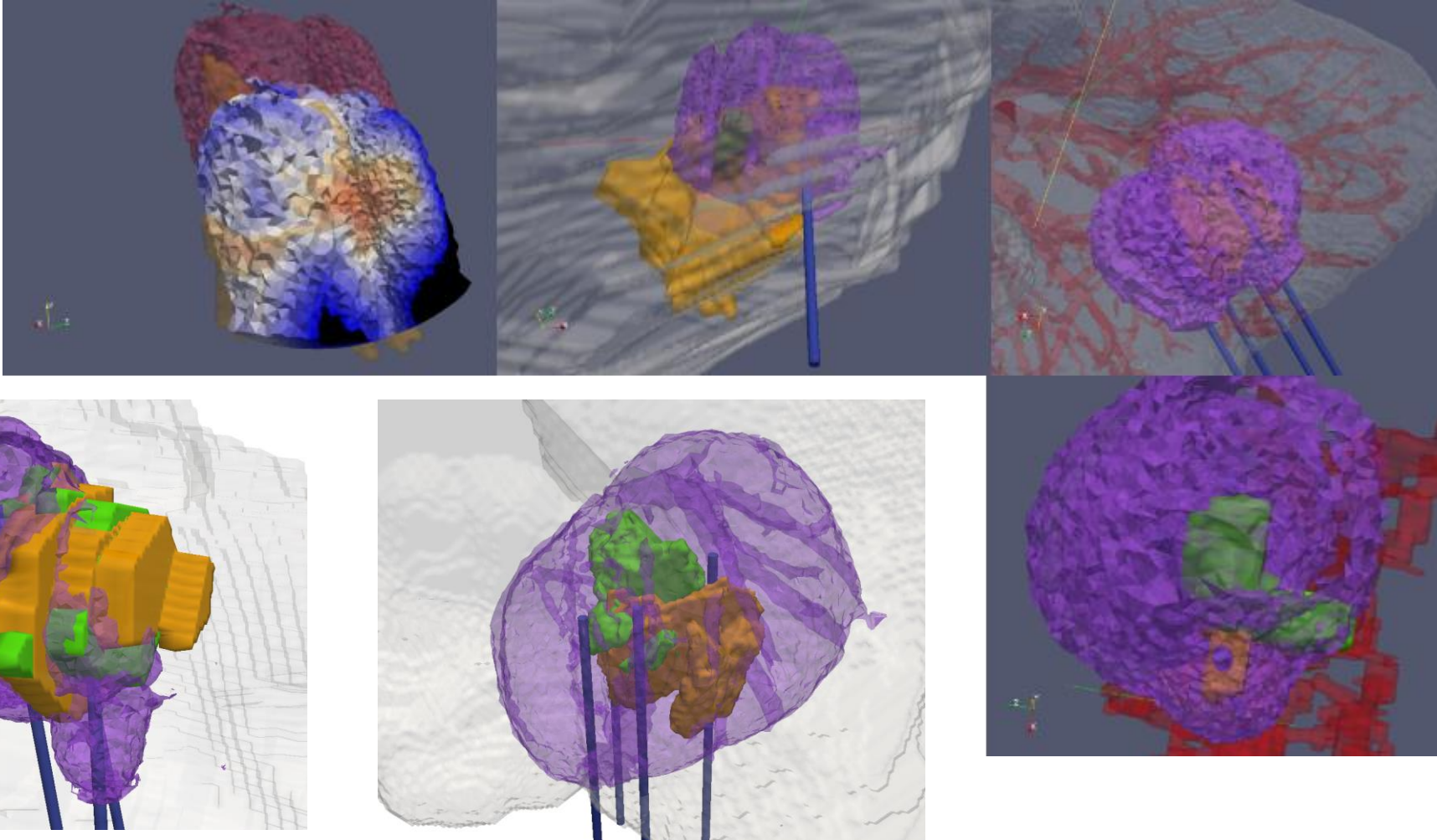
IRE

- Location of varying tissue types
 - Based on existing models,
 - observable effect of tumour
- Effects of almost-parallel placement
 - under/over-treatment at ends
 - rounding off at mismatching tips
 - selecting representative axis
- Accurately modelling effects of altering pulse duration, pulse length and capturing active length of needle



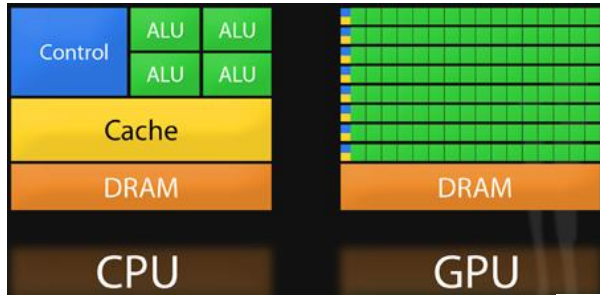
Generic Open-end Simulation, Environment for Minimally Invasive Cancer Treatment

IRE



Summary

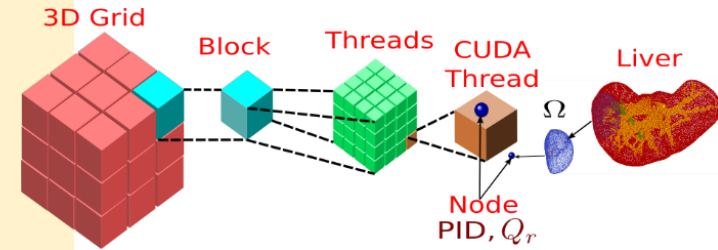
Computations in GPU



- CPU does**
- ✘ Mesh generation
 - ✘ Receives mesh
 - ✘ Generates neighbours
 - ✘ Constructs the initial CSR matrix



- Each node requires**
- ✘ PID controlled power input
 - ✘ Source term (Q_r)
- Each thread of GPU computes**
- Each Node's**
- ✘ PID controlled power input
 - ✘ Source term

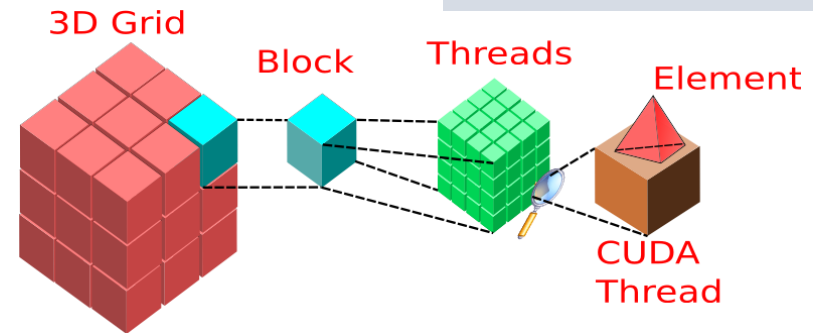


- Each element requires**
- ✘ 4 x 4 matrix inversion
 - ✘ Stiffness matrix construction
 - ✘ Mass matrix construction
 - ✘ Volume computation

- Each thread of GPU computes**
- each Element's**
- ✘ 4 x 4 matrix inversion
 - ✘ Stiffness matrix
 - ✘ Mass matrix
 - ✘ Volume

	0	1	2	3	4
0	2.0		3.5		6.7
1		8.2		9.2	
2		1.1	2.8		
3	3.0		1.5	4.5	
4		2.5		8.9	

	0	1	2	3	4	5						
rowptr	0	3	5	7	10	12						
colind	0	2	4	1	3	1	2	0	2	3	1	3
values	2.0	3.5	6.7	8.2	9.2	1.1	2.8	3.0	1.5	4.5	2.5	8.9



Linear Solver and Assembly



Assembly

- ✘ Stiffness matrix assembled directly to CSR matrix
- ✘ Neighbour map algorithm between stiffness matrix and CSR matrix



ILU Precondition BICGSTAB



CUDA Libraries



ILU Computation using CUSPARSE¹ library



Each solver operation uses CUBLAS¹ and CUSPARSE¹ libraries



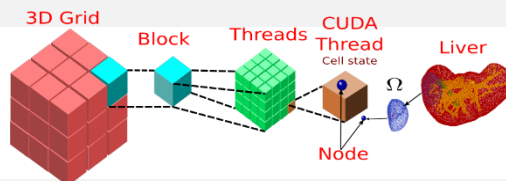
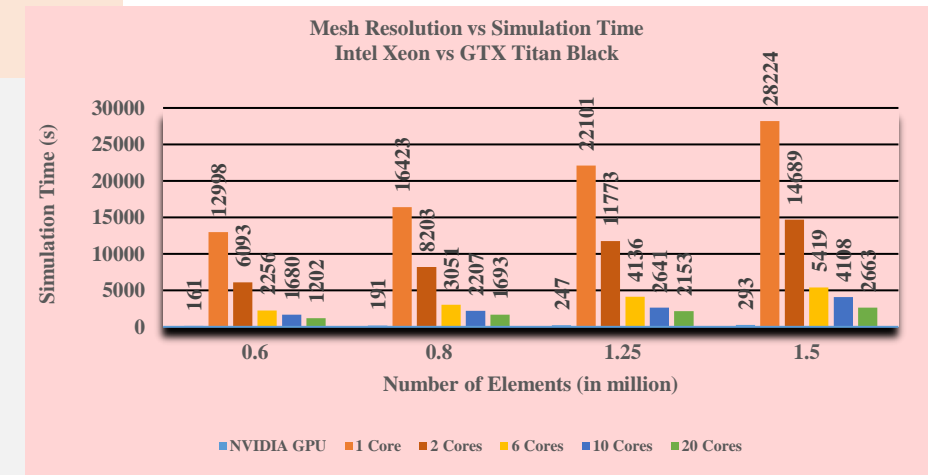
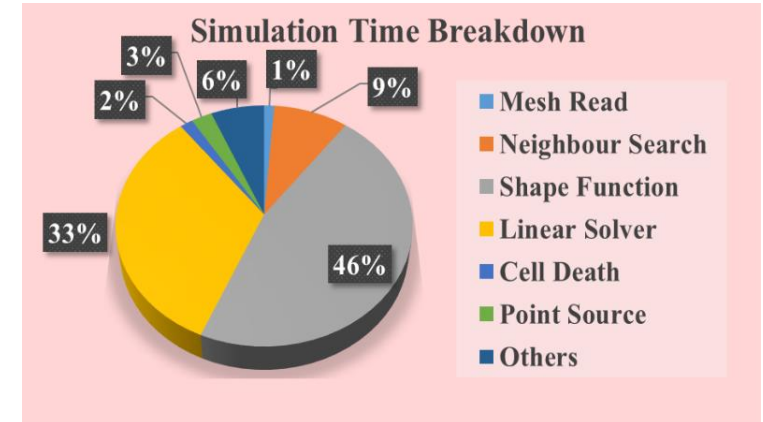
Each **node** requires

- ✘ Dead state
- ✘ Alive state
- ✘ Blood Perfusion value
- ✘ Specific heat capacity value



Each **thread** of GPU computes each **node's**

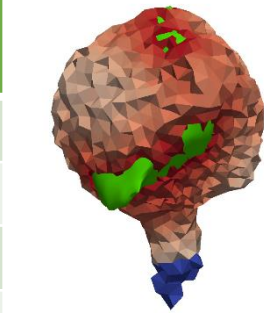
- ✘ Dead state
- ✘ Alive state
- ✘ Blood Perfusion value
- ✘ Specific heat capacity value



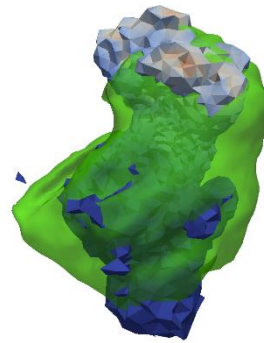
¹NVIDIA Corporation (2015), CUDA C Programming guide, Version 7.5

Simulation Speedup

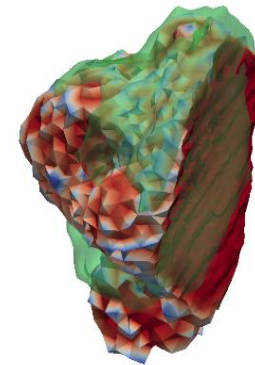
Pat.	# Abl.	RFA Real duration (minutes)	Perfusion $\frac{ml}{100ml \text{ min}}$	Sim. Time (sec)
4	1	18	21.6, 21.6	104
5	2	28	0, 0	103
6	2	11	36, 21.6	73
7	2	19	21.6, 36	115
8	2	29	105.6, 36	188
9	1	12	36, 21.6	64



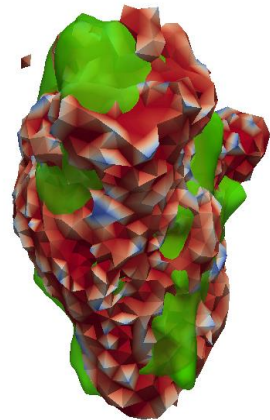
RVD: 18
Surf Dev: 2.28



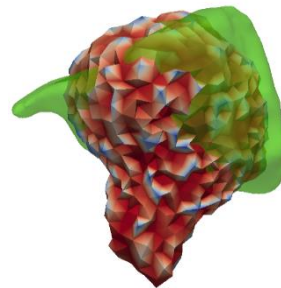
RVD: 74
Surf Dev: 3.09



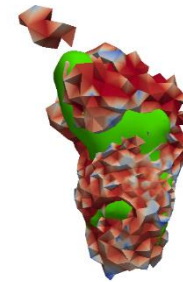
RVD: 6.67
Surf Dev: 2.88



RVD: 0.003
Surf Dev: 4.57



RVD: 0.61
Surf Dev: 2.74



RVD: 55.71
Surf Dev: 1.88

Pat.	# Abl.	RFA Real duration (minutes)	Perfusion $\frac{ml}{100ml \text{ min}}$	Sim. Time (sec)
10	1	13	125, 125	70
11	2	32	110, 40	137
12	3	62	68.9, 70	322
13	1	9	85, 25	44
14	2	15	95, 60	95
15	3	14	135, 0	92
16	3	53	140, 45	313
17	3	62	60, 0	323
18	2	26	132, 36	150
19	1	11	57, 36	83
20	1	8	47, 36	34
21	1	12	40, 36	53

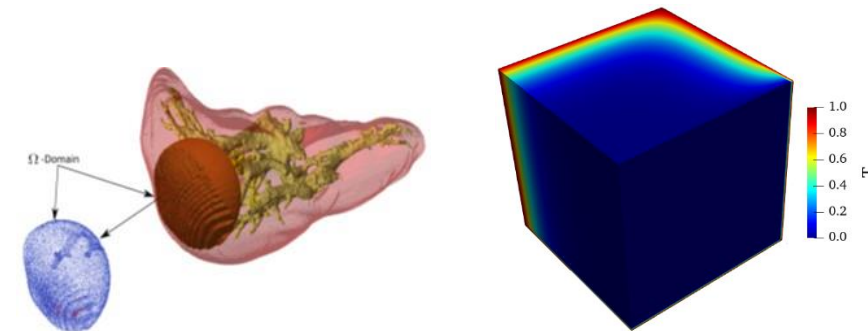
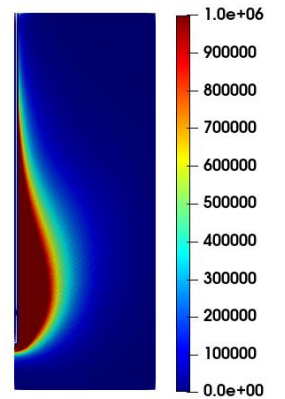
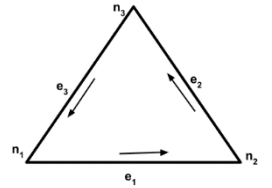
$$DICE = \frac{2|V_{se} \cap V_{si}|}{|V_{se}| + |V_{si}|}$$

$$RVD = \left| \frac{|V_{se}|}{|V_{si}|} - 1 \right|$$

$$Volume \ overlap = \frac{|V_{si} \cap V_{se}|}{|V_{si} \cup V_{se}|}$$

Accepted:
Surface deviation < 3.5mm
RVD < 20 %

- ❖ GPU accelerated MWA Solver for online computing
- ❖ Vector Finite Element Method for Microwave Ablation
- ❖ Finite Pointset based simulation of FSI problems of RFA Treatment



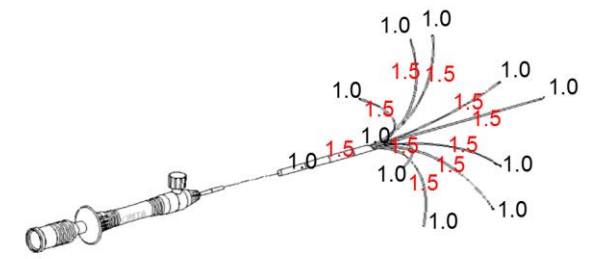
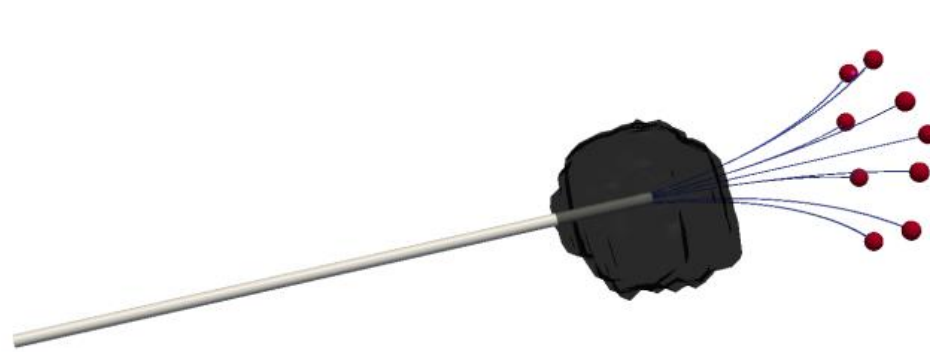
- ❖ A maximum of **6 minutes** computation time for an hour protocol
- ❖ If machines are available with 4GPUs on a PC with super cooling fan, it is possible to run 4 simulations at the same time by changing parameters such as GPU and port numbers
 - ❖ 20-20-20: 20 simulations for a 20 minutes protocol could be done in 20 minutes
- ❖ Provides good accuracy with less than 2.5mm surface deviation error
- ❖ RVD average: 17.99%

This presentation: based on the following articles:

Panchatcharam Mariappan, P. Weir, R. Flanagan, et al, ***GPU-based RFA Simulation for minimally invasive cancer treatment of liver tumours***, International Journal of Computer Assisted Radiology and Surgery, 12(1): 59-68, 2017

Panchatcharam M, Phil W and Ronan F, GPU accelerated finite element method for radiofrequency ablated cancer treatment, *PRACE DAYS 2015*, May 2015: **Best Poster Presentation Award**

1. Gangadhara B, **Panchatcharam M**, A Vector Finite Element Approach to Temperature Dependent Parameters of Microwave Ablation for Liver Cancer, *International Journal for Numerical Methods in Biomedical Engineering*, 2023
2. **Panchatcharam M**, Gangadhara B, Ronan F, A Point Source Model to Represent Heat Distribution Without Calculating the Joule Heat during Radiofrequency Ablation, *Frontiers in Thermal Engineering*, 2022
3. Cindric H, **Panchatcharam M**, Beyer L, Wiggermann P and Moche M, Miklavcic D and Kos B, Retrospective study for validation and improvement of numerical treatment planning of irreversible electroporation ablation for treatment of liver tumors, *IEEE Transactions on Biomedical Engineering*, 2021.
4. Martin J.A, **Panchatcharam M**, Philip V, Ronan F, Sjoerd F. M. J, Mika P, Marina K, Michael M and Jurgen F, Software-based planning of ultrasound and CT-guided percutaneous radiofrequency ablation in hepatic tumors, *International Journal of Computer Assisted Radiology and Surgery*, 16, pp. 1051-1057, 2021
5. Tim Van O, Jan H, Michael M, Phil W, **Panchatcharam M**, Ronan Flanagan, Mika P, Stephen P, Marina K, Sjoerd, F. M. J and Jurgen F, Validation of a web-based planning tool for percutaneous cryoablation of renal tumors, *CardioVascular and Interventional Radiology*, September 2020 (IF: 0.67)
6. Michael M, Harald B, Jurgen F, Camila A H, Daniel S, Philipp B, Marina K, Sjoerd J, Roberto B S, Gaber K, Mika P, Martin E, Horst R P, Philip V, Ronan F, **Panchatcharam M** and Martin R, *Clinical evaluation in silico planning and real-time simulation of hepatic radiofrequency ablation (ClinicIMPACT Trial)*, *European Radiology*, 30, 934-942, 2020. (IF: 4.101)
7. Philip V, **Panchatcharam M**, Mika P, Ronan F, Roberto B s, Rupert H P, Jurgen F, Dieter S, Marina K and Michael M, *RFA Guardian: Comprehensive simulation of radiofrequency ablation treatment of liver tumors*, *Nature Scientific Reports*,8(1), 2018. (IF: 4.529)
8. Martin R, Philip B, Daniel S, Marina K, Sjoerd J, Roberto B. S, Martin E, Philip V, Ronan F, **Panchatcharam M**, Harald B and Micahel M, *A prospective development study of software-guided radio-frequency ablation of primary and secondary liver tumors: Clinical intervention modeling, planning and proof for ablation cancer treatment (ClinicIMPACT)*, *Contemporary Clinical Trials Communications*, 8, 25-32, 2017. (IF: 1.935)
9. **Panchatcharam M**, Phil W, Ronan F, Philip V, Tuomas A, Mika P, Michael M, Harald B, Jurgen F, Horst R P, Roberto B S and Marina K, *GPU-based RFA simulation for minimally invasive cancer treatment of liver tumours*, *International Journal of Computer Assisted Radiology and Surgery*, 12(1): 59-68, 2017 (IF: 1.707)



End of Lecture

